AFCRL 933

Scientific Report 2

INVESTIGATION OF A SQUARE-MESH WIRE-GRID MODIFIED-LUNEBURG-LENS ANTENNA

Prepared for:

ELECTRONICS RESEARCH DIRECTORATE
AIR FORCE CAMBRIDGE RESEARCH LABORATORIES
OFFICE OF AEROSPACE RESEARCH
UNITED STATES AIR FORCE
BEDFORD, MASSACHUSETTS

CONTRACT AF 19(604)-8059

By: *M. G. Andreasen* *R. L. Tanner*

STANFORD RESEARCH INSTITUTE
MENLO PARK, CALIFORNIA

*SRI

Requests for additional copies by Agencies of the Department of Defense, their contractors, and other Government agencies should be directed to the:

ARMED SERVICES TECHNICAL INFORMATION AGENCY
ARLINGTON HALL STATION
ARLINGTON 12, VIRGINIA

Department of Defense contractors must be established for ASTIA services or have their "need-to-know" certified by the cognizant military agency of their project or contract.

All other persons and organizations should apply to the:

U.S. DEPARTMENT OF COMMERCE
OFFICE OF TECHNICAL SERVICES
WASHINGTON 25, D.C.

STANFORD RESEARCH INSTITUTE
MENLO PARK, CALIFORNIA

September 1961

AFCRL 933

Scientific Report 2

INVESTIGATION OF A SQUARE-MESH WIRE-GRID MODIFIED-LUNEBURG-LENS ANTENNA

Prepared for:

ELECTRONICS RESEARCH DIRECTORATE
AIR FORCE CAMBRIDGE RESEARCH LABORATORIES
OFFICE OF AEROSPACE RESEARCH
UNITED STATES AIR FORCE
BEDFORD, MASSACHUSETTS

CONTRACT AF 19(604)-8059

By: *M. G. Andreasen* *R. L. Tanner*

SRI Project No. 3619

Approved:

D. R. SCHEUCH, DIRECTOR ELECTRONICS AND RADIO SCIENCES DIVISION

Copy No. 38

ABSTRACT

This report describes the design, construction and measured performance of an experimental square-mesh wire-grid modified Luneburg lens antenna. This novel antenna shows great promise for many applications. The lens part of the experimental antenna consists of a ground plane above which is placed a circular square-mesh wire-grid whose distance from the ground plane is varied so as to achieve a focusing effect. The lens is loaded with a radial horn to obtain a high radiation efficiency. The lens antenna was tested with an omnidirectional feed and with a directional feed in a bandwidth of more than 2:1. The measured radiation patterns agree very well with the theoretical patterns. With a simple directional feed, side-lobe levels of below -20 db were obtained.

CONTENTS

ILLUSTRATIONS

I INTRODUCTION

Circularly symmetric lenses with a varying index of refraction, e.g. the Luneburg lens,[1-4]* are very useful for large directional antennas whose beams must be scanned through 360° in azimuth at a very high rate. With many feeds placed along the rim of the lens, the beam of the lens antenna can be scanned electrically by switching the transmitter or the receiver from feed to feed.

The greatest problem in exploiting the circularly symmetric lens for a beam-scanning antenna is to find a suitable material for constructing the lens. Both real dielectrics and artificial dielectrics have been used at microwave frequencies, although they are only marginally practical. At frequencies below the microwave spectrum, however, they become wholly impractical.

At microwave frequencies, most circularly symmetric lens antennas have been designed using parallel-plate techniques.[5-7] Parallel-plate lenses are often quite frequency-sensitive because of the dispersive character of the wave propagated between the plates, and they become impractical at frequencies below the microwave region. A surface-wave structure[8] could be used for lens designs at lower frequencies, although its strong frequency dependence is quite limiting.

A structure that has potential applications for beam-scanning lens antennas, at both microwave and lower frequencies, and that has broadband properties was invented some years ago by R. L. Tanner[9]. This structure consists of a pair of wire grids with square, triangular, or hexagonal mesh. The feature of a pair of wire grids that makes it useful for lens designs is that the phase velocity of a quasi-TEM-wave propagating between the grids is a function of the ratio between the grid-to-grid spacing and the mesh size. When the grids are very close together, the wave velocity is $1/\sqrt{2}$ times the velocity of light. When, on the

---

* References are listed at the end of the report.

other hand, the grids are far apart, the wave velocity approaches the velocity of light. The grid-structure can be made as broadband as is desired by using a sufficiently small mesh.

The grid structure is expected to be particularly important to the design of lens antennas in the HF band, where no partically useful structure has hitherto been known. Using an extremely broadband antenna to feed the lens, a grid-type HF lens antenna can be designed to cover the entire HF band. Although the HF lens antenna lends itself naturally to use as a high-resolution direction finder, it is equally useful in communication. In communication applications, one grid-type lens antenna can be operated on as many simultaneous channels as desired throughout the entire HF band and in any desired direction.

At microwave frequencies, where parallel-plate techniques have thus far been predominant in lens designs, the grid structure should prove very useful. One form of a microwave grid-type lens would consist of a sheet of dielectric with a metal grid printed on each side of the sheet. The required variation of the ratio between the grid-to-grid spacing and the mesh size can be achieved by using a dielectric sheet of constant thickness and changing only the mesh size of the grid. Alternatively, the mesh size can be kept constant and the width of the strip conductors forming it can be varied. Such a lens would be very simple to fabricate and tolerances wo· d present no problem. Eventually, one of the grids could be replaced by a conducting plate.

Significant results for the design of a grid-type lens antenna have already been achieved by Stanford Research Institute on AFCRL Contract AF 19(604)-2240.[10-11] The purpose of the work done on that contract was to obtain theoretical and experimental design information for a square-mesh grid-type lens, and to investigate the properties of a radial horn that is attached to a circularly symmetric lens to increase the radiation efficiency of the lens itself. The radial horn acts as a broadband transformer between the lens and free space. Using the design data previously derived for a pair of square-mesh wire grids, an experimental model of a grid-type lens antenna has been constructed and tested

on the present contract. The design and the theoretical and measured performance of this lens antenna will be described in the following sections.

II DESIGN AND CONSTRUCTION OF AN EXPERIMENTAL GRID-TYPE LENS ANTENNA

Using the information already available on the equivalent dielectric constant of a pair of square-mesh wire-grids[10-11] an experimental lens antenna was designed and constructed. For convenience, the theoretical equivalent static dielectric constant of a square-mesh wire-grid placed parallel to a conducting plane is reproduced in Fig. 1. The curves show the equivalent dielectric constant as a function of the ratio between the grid-to-ground spacing a and the mesh size b for various values of the ratio between the mesh size b and the wire radius r_o .

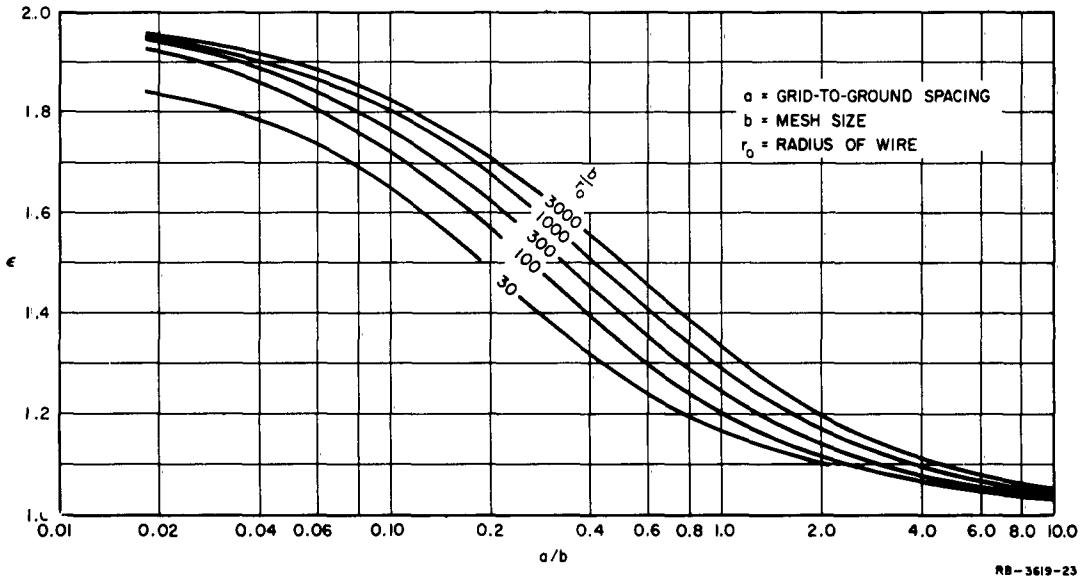

FIG. 1 EQUIVALENT STATIC DIELECTRIC CONSTANT OF A SQUARE-MESH WIRE GRID PLACED ABOVE A GROUND PLANE vs. THE RATIO BETWEEN THE GRID-TO-GROUND SPACING AND THE MESH SIZE FOR VARIOUS VALUES OF b/r_0

A photograph of the experimental lens antenna is shown in Fig. 2. The antenna consists of an 8-foot-diameter ground plane above which is placed a 5-foot-diameter aluminum ring that supports a square-mesh wire grid. A metallic radial horn is attached to the grid ring to provide a high radiation efficiency of the antenna.

The polarization of the radiation field in the azimuth plane is vertical, and hence perpendicular to the ground plane of the lens antenna.

The wire used for the grid is a 0.016-inch-diameter silver-coated beryllium copper wire, and the grid mesh size is 0.75 inch. With this mesh size, the lens should operate without notable dispersion or anisotropy effects up to a frequency of close to 2000 Mc.[10,11] At 2000 Mc, the mesh size is one-eighth wavelength.

The grid was woven over a conic frustum so that, when soldered to the 5-foot-diameter ring, the grid would sag somewhat. The ring holding the grid was placed at a constant spacing of 2.5 inches from the ground plane by means of a number of thin dielectric spacers. The correct shape of the grid was achieved by pulling the grid down to the correct distance from the ground plane and holding it in position by nylon thread fastened to the ground plane. At a certain stage during the radiation pattern measurements, the performance of the lens antenna started to deteriorate. This deterioration was traced to the combined stretching and loosening of the nylon thread that was supposed to hold the grid in the correct shape. After small pieces of polyfoam were put under the grid and the grid was retied to the correct shape, the original electrical performance of the antenna was restored. The polyfoam pieces have a negligible effect upon the electrical performance of the antenna.

The performance of the antenna should not be much affected whether the radial horn is made of sheet metal or whether it is made as a wire grid. For ease of construction, the horn was, therefore, made of an aluminum sheet and screwed to the ring holding the wire-grid lens.

The experimental grid-type lens was not designed as a Luneburg lens, because a Luneburg lens requires a maximum dielectric constant of 2 in the center of the lens. Although the wire-grid structure theoretically

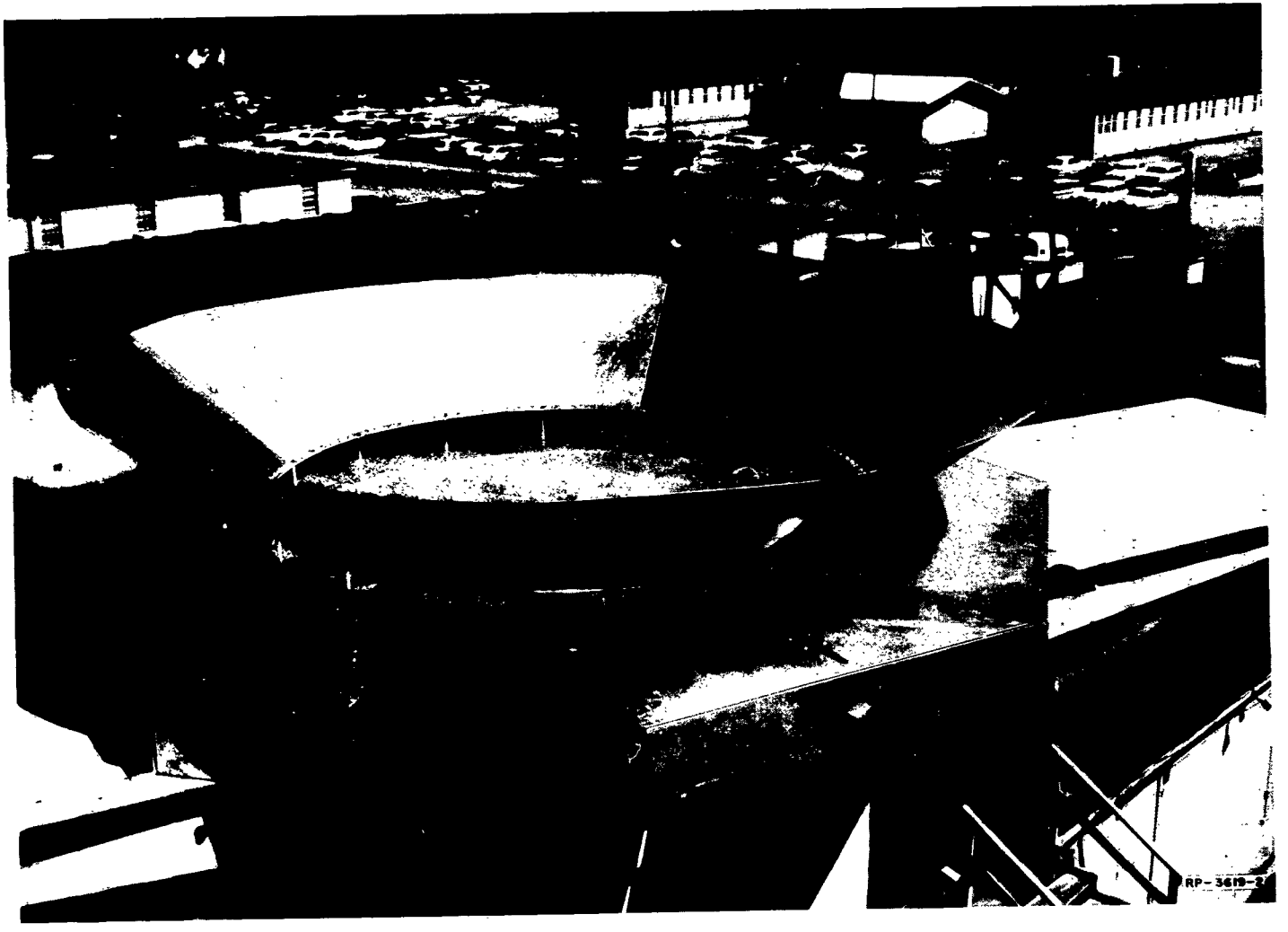

FIG. 2 PHOTOGRAPH OF EXPERIMENTAL SQUARE-MESH WIRE-GRID LENS ANTENNA

has an equivalent dielectric constant of 2 when the grid-to-ground spacing is very much smaller than the mesh size, it is more advantageous in practice to design a grid-type lens as a modified Luneburg lens that is fed from a source outside of the lens and has a maximum dielectric constant that is less than 2 . The smaller maximum dielectric constant in the center of the lens makes tolerances for the grid-to-ground spacing at the center of the lens less severe, and increases the power capacity of the lens, which is an important factor for high-power transmitting antennas. Also, by moving the lens feed outside the lens, that is, into the radial horn, less aperture blocking will be encountered than if the feed were placed at the rim of the lens.

A modified Luneburg lens for a defocused source has been analyzed by Cheng.[12] To achieve a condition such that all rays entering a circularly symmetric lens from a source placed outside of the lens shall be parallel after leaving the lens, the equivalent dielectric constant of the lens must, according to Cheng, satisfy the relation

$$\epsilon = \left(1 + \sqrt{1 - \epsilon\left(\frac{r}{f}\right)^2}\right) e^{-\frac{2}{\pi}\int_1^f \frac{\text{Arc sin}\left(\frac{t}{f}\right)}{\sqrt{t^2 - \epsilon r^2}}\, dt} \qquad (1)$$

where the lens radius has been normalized to the value 1 (see Fig. 3). Here, r is the distance from the center of the lens to the point of the lens where ϵ is evaluated, and f is the distance from the center of the lens to the source ($f > 1$). As acknowledged by Cheng,[12] the integral in this expression has not been evaluated in closed form. The integral can, however, be evaluated approximately. Assuming that f is only a little larger than 1 , the function Arc sin $\left(\frac{t}{f}\right)$ can, with reasonable accuracy, be approximated by $\frac{\pi}{2}$ in the integration interval $1 \leqq t \leqq f$. A similar reduction of the denominator of the integral is

not permissible. With the above approximation we find

$$\epsilon = \left(1 + \sqrt{1 - \epsilon\left(\frac{r}{f}\right)^2}\right) e^{-\ln\left(f\,\frac{1+\sqrt{1-\epsilon\left(\frac{r}{f}\right)^2}}{1+\sqrt{1-\epsilon\, r^2}}\right)} \tag{2}$$

from which it follows that

$$\epsilon = \frac{2}{f} - \left(\frac{r}{f}\right)^2 . \tag{3}$$

This is of a parabolic form.

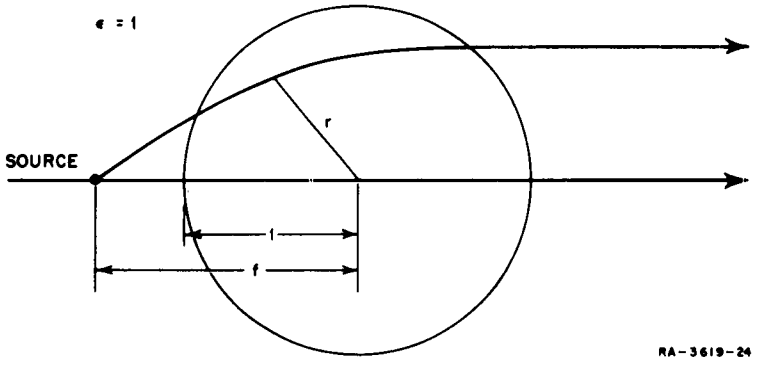

FIG. 3 MODIFIED LUNEBURG LENS FOR DEFOCUSED SOURCE

We shall estimate the accuracy of this expression by comparing the values obtained from this expression with more accurate values for $r = 0$ and $r = 1$. For $r = 1$ we find

$$\epsilon = \frac{2}{f} - \frac{1}{f^2}$$

while the correct value is known to be $\epsilon = 1$. The relative error is

$$\frac{\Delta\epsilon}{\epsilon} = \frac{(f-1)^2}{2f-1} \tag{4}$$

and is small (of second order in $f - 1$).

For $r = 0$, we find from Eq. (3)

$$\epsilon = \frac{2}{f} \ .$$

A more accurate expression for $r = 0$ can be found from Eq. (1) by using the approximation formula

$$\text{Arc sin } x \approx \frac{\pi}{2} - \sqrt{2(1-x)}$$

which is valid when x is close to 1 . We find then for $r = 0$

$$\epsilon = \frac{2}{f}\, e^{\frac{\sqrt{2}}{\pi}\left(\frac{f-1}{f}\right)^2} \approx \frac{2}{f}\left[1 + \frac{\sqrt{2}}{\pi}\left(\frac{f-1}{f}\right)^2\right] . \tag{5}$$

The relative error is thus

$$\frac{\Delta\epsilon}{\epsilon} = \frac{\frac{\sqrt{2}}{\pi}\left(\frac{f-1}{f}\right)^2}{1 + \frac{\sqrt{2}}{\pi}\left(\frac{f-1}{f}\right)^2} \tag{6}$$

which is seen to be small (of second order in $f - 1$).

We can improve on the accuracy of Eq. (3) by letting ϵ remain of parabolic form in r , but requiring that the improved expression for ϵ

give the more correct values of ϵ for $r = 0$ and $r = 1$. Accordingly, we find

$$\epsilon = \frac{2}{f} e^{\frac{\sqrt{2}}{\pi}\left(\frac{f-1}{f}\right)^2} - \left[\frac{2}{f} e^{\frac{\sqrt{2}}{\pi}\left(\frac{f-1}{f}\right)^2} - 1\right] r^2 . \qquad (7)$$

This expression was used in designing the experimental wire-grid lens. The curves in Fig. 4 show the dielectric constant as a function of r for various values of f. These curves were computed from Eq. (7).

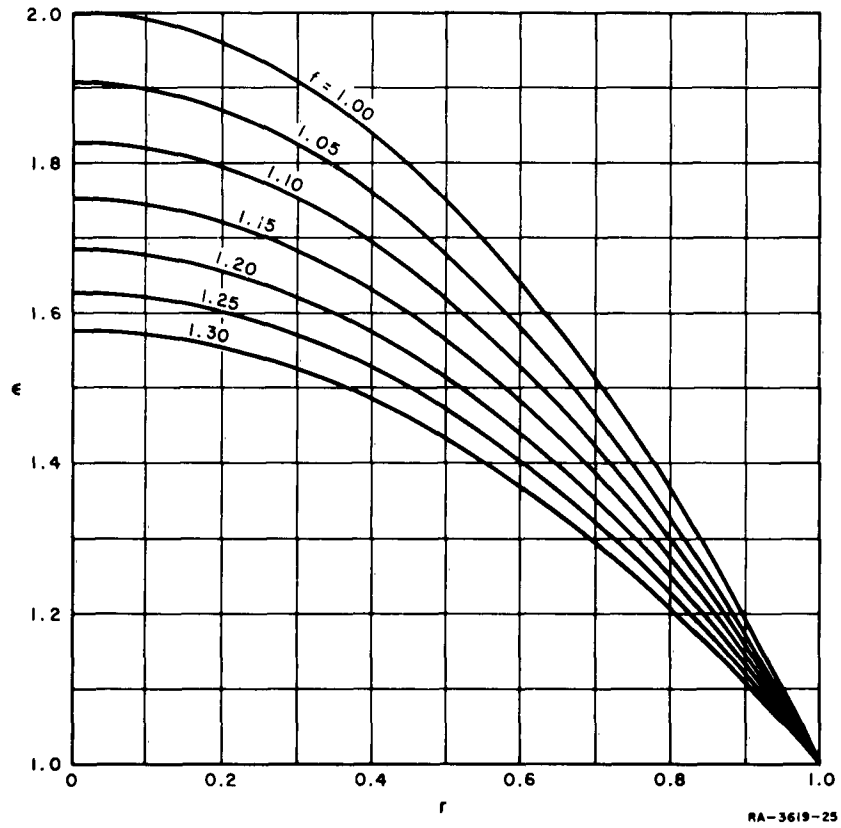

FIG. 4 EQUIVALENT DIELECTRIC CONSTANT OF MODIFIED LUNEBURG LENS FOR DEFOCUSED SOURCE vs. THE NORMALIZED RADIAL COORDINATE FOR VARIOUS NORMALIZED DISTANCES, f, FROM THE SOURCE TO THE CENTER OF THE LENS

In the experimental wire-grid lens, the closest spacing between the grid and the ground plane, occurring at the center of the lens, was chosen to be 0.075 inch. Since the chosen mesh size was 0.750 inch, and the wire radius is 0.008 inch, we have $\frac{a}{b} = 0.1$ and $\frac{b}{r_o} = 94$ at the center of the lens. Entering Fig. 1 with these values of $\frac{a}{b}$ and $\frac{b}{r_o}$, we find the maximum equivalent dielectric constant to be 1.71 at the center of the lens. According to Eq. (7), the variation of the dielectric constant throughout the lens will therefore be

$$\epsilon = 1.71 - 0.71\, r^2 \tag{8}$$

The required distance from the center of the lens to the source is now found to be, from Eq. (7),

$$f = 1.18 \ .$$

The radius of the experimental wire-grid lens is 30 inches. The phase center of the source for the lens should therefore be $30 \times 1.18 \approx 35.5$ inches away from the center of the lens. The measurements on the lens antenna that will be described in Sec. IV proved that this feed position was very nearly optimum. As shown in Fig. 2, two slots were cut in the ground plane. One slot points in the direction of one set of parallel wires of the grid; the other slot points in the diagonal direction of the grid. The feed antenna, which is not shown in the photograph, was mounted in one of the slots so that it could be moved back and forth along the slot.

The required shape of the wire grid can be predicted from Eq. (8) and the curves in Fig. 1; it is shown as the solid curve in Fig. 5. The shape, given as the spacing between the grid and the ground plane vs. the radial coordinate, is shown on a logarithmic scale because of the large range of the grid-to-ground spacing. It is noted that the grid-to-ground spacing must theoretically approach infinity at the rim of the lens. This is necessary because the phase velocity of a

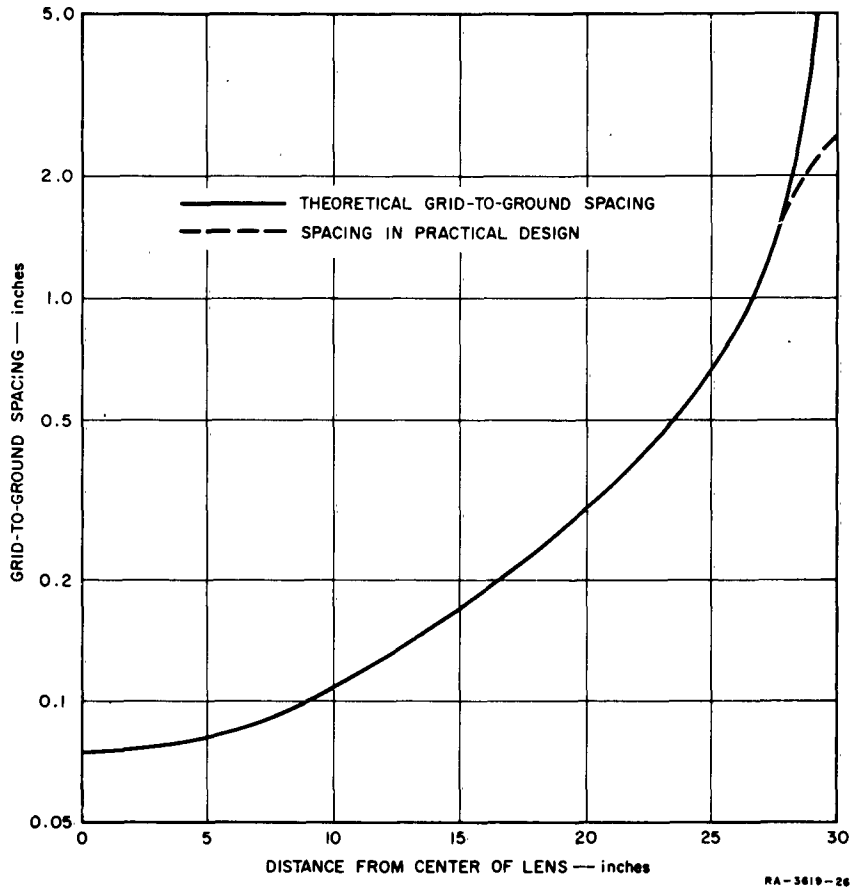

FIG. 5 GRID-TO-GROUND SPACING OF EXPERIMENTAL WIRE-GRID LENS ANTENNA

plane wave propagating in the grid-to-ground region will always be less than the velocity of light, no matter how large the grid-to-ground spacing is. For a practical design, the theoretical grid shape shown by the solid curve in Fig. 5 near the rim of the lens can be replaced by the shape shown by the dotted curve without any appreciable change in the expected performance of the lens. The dotted curve is actually a straight line tangent to the theoretical curve. With a grid-to-ground spacing of 2.5 inches at the rim of the lens, the equivalent dielectric constant at the rim of the lens is 1.07, according to Fig. 1, in contrast to the theoretically desirable value of 1. Because of the higher

dielectric constant near the rim of the lens, the field in a plane aperture in front of the lens will not have constant phase near the edges of this aperture. For the experimental lens, the phase distortion is only 30 degrees at the edges of the aperture at a frequency of 1 Gc. The region near the edges of the aperture where this phase distortion exists occupies only about 5 percent of the total aperture and will often be weakly illuminated. For these reasons, the higher dielectric constant at the rim of the experimental lens is not expected to change the performance of the lens appreciably.

The bandwidth of a square-mesh wire-grid lens is limited because of anisotropy and dispersion effects that become important when the mesh size is no longer very much smaller than the wavelength. Using existing experimental information on the anisotropy and dispersion of a pair of square-mesh wire grids,[10,11] an estimate can be made of the upper frequency limit of a square-mesh wire-grid lens. According to Eq. (7), the equivalent dielectric constant of the lens can be written

$$\epsilon_{st} = \epsilon_{max} - (\epsilon_{max} - 1)\left(\frac{r}{R_o}\right)^2 \tag{9}$$

where ϵ_{max} is the equivalent dielectric constant at the center of the lens. The above reported measurements[10,11] showed that the equivalent dielectric constant of the lens increases most rapidly with frequency for propagation along the wires of the grid. It is therefore anticipated that the most serious phase-distortion effects will occur when the principal direction of the lens antenna is parallel to one set of wires of the grid. Thus, assuming that the electrical path length of a ray passing close to the rim of the lens is proportional to the free-space propagation constant, the maximum phase error in the plane aperture in front of the lens is determined from the electrical path length of a ray passing through the center of the lens. According to the measurements reported above[10,11], the equivalent dielectric constant of the lens can roughly be described

by the relation

$$\epsilon = \epsilon_{st} (1 + \Delta) \tag{10}$$

where Δ is a frequency-dependent correction factor that is nearly proportional to the square of the mesh size measured in wavelengths; that is,

$$\Delta = \kappa \left(\frac{b}{\lambda} \right)^2 . \tag{11}$$

where κ is a frequency-independent proportionality constant. Using Eq. (7), we now find that the electrical path length in the lens of a ray passing through the center of the lens is

$$\Phi = k R_o \sqrt{1 + \Delta} \left(1 + \frac{\epsilon_{max}}{\sqrt{\epsilon_{max}^{-1}}} \text{ Arc sin} \sqrt{\frac{\epsilon_{max}^{-1}}{\epsilon_{max}}} \right) \text{ radians} \tag{12}$$

where k is the free-space propagation constant, and R_o is the lens radius. The maximum phase error in a plane aperture in front of the lens is therefore approximately

$$\Delta\Phi = \frac{\Delta}{2} k R_o \left(1 + \frac{\epsilon_{max}}{\sqrt{\epsilon_{max}^{-1}}} \text{ Arc sin} \sqrt{\frac{\epsilon_{max}^{-1}}{\epsilon_{max}}} \right) \text{ radians} \tag{13}$$

To avoid an appreciable effect of this phase error upon the side-lobe level of the lens radiation pattern, it is reasonable to prescribe that this phase error not exceed 1 radian. Introducing Eq. (11) in Eq. (13), we finally find the following expression for the minimum wavelength at

which the lens can be operated:

$$\lambda_{min} = \sqrt[3]{\pi R_o b^2 \kappa \left(1 + \frac{\epsilon_{max}}{\sqrt{\epsilon_{max} - 1}} \text{ Arc sin } \sqrt{\frac{\epsilon_{max} - 1}{\epsilon_{max}}}\right)} \quad . \qquad (14)$$

It should be pointed out that in the derivation of this expression it has been tacitly assumed that the lens aperture efficiency is high, that is, that the feed is not too directional. For some applications, such as a broadband HF communication antenna, however, it may be desired that the beamwidth of the lens radiation pattern be fairly independent of frequency. This can be achieved by lowering the lens aperture efficiency, that is, by increasing the feed directivity with increasing frequency. In such a case, the minimum operating wavelength is lower than predicted by Eq. (14) by a factor considerably higher than 1.

For the constructed experimental lens ($\epsilon_{max} = 1.71$; $R_o = 30$ inches; $b \doteq 0.75$ inch; $\kappa = 3$) we find from Eq. (14) $\lambda_{min} = 7$ inches, corresponding to a maximum operating frequency of $f_{max} = 1700$ Mc. The measurements described in Sec. IV show that the experimental lens antenna can be operated up to a frequency of approximately 1750 Mc when the feed has little directivity. With a more directive feed, the lens can probably be used up to about 3000 Mc.

Theoretically, there is no lower frequency limit of the lens. However, in order that the radial horn act as an efficient transformer between the lens and free space, it is necessary that the height of the horn aperture be at least one wavelength. Since the aperture height of the experimental lens antenna is 16 inches, this makes the lower frequency limit of the experimental antenna 740 Mc. The experimental antenna was tested down to a frequency of 750 Mc and at this frequency was found to ope ate relatively well.

III THEORETICAL RADIATION PATTERNS OF A MODIFIED LUNEBURG LENS WITH VARIOUS FEEDS

Radiation patterns of a Luneburg lens fed by an omnidirectional feed, a dipole-type feed and a cardioid-type feed have been calculated by Jasik.[8] No calculations seem to have been carried through for radiation patterns of a modified Luneburg lens with a feed displaced from the rim of the lens, or for a general type of feed pattern. Since such calculations would be very valuable for designing a grid-type lens antenna, we shall in this section investigate theoretically the radiation pattern of a modified Luneburg lens with a feed whose pattern belongs to a class of patterns all characterized by the value of a single parameter.

To determine the radiation field of a modified Luneburg lens, we shall assume that the lens diameter is large compared to one wavelength. With this assumption we can easily, and with reasonable accuracy, predict the field at the rim of the lens by geometrical optics. The radiation field of the lens can be calculated from the field at the rim of the lens by various methods.

It has previously been shown[10] that the ideal horizontal radiation pattern of the lens is only slightly modified by the radial horn that is assumed to be attached to the lens to achieve a high radiation efficiency. In the following calculations of the horizontal radiation pattern of a lens, we can therefore neglect any effect of the radial horn upon the radiation pattern and assume that the lens radiates into a parallel-plate region, or, what theoretically amounts to the same thing, we can assume that the antenna is two-dimensional.

The relative horizontal radiation pattern arising from the field at the rim of the lens can be calculated by expressing the field in space as a sum of cylindrical wave functions. The amplitudes of these wave functions can be found by matching the total field to the known field at the rim of the lens and will be given in terms of cylindrical Hankel functions. The number of wave functions that must be taken into account

to determine the radiation field with reasonable accuracy will be of the order of the number of wavelengths measured along the circumference of the rim of the lens. Although numerical computations can be somewhat simplified by approximating the Hankel function by the WKB-method,[10] the usual computation time involved remains relatively large for a large lens. This method of finding the radiation field should only be used when extremely accurate results are desired.

When the radiation pattern of the feed is of a certain type, the radiation pattern of the lens can more easily be determined by Huyghens' principle. Using Huyghens' principle, the radiation field of the lens will be given in terms of a transform of the field at the rim of the lens which takes the form of an integration along the rim of the lens. However, the integral along the circular rim of the lens is usually rather difficult to evaluate in closed form. For this reason, we shall further assume that we can use geometrical optics to predict the field in a plane aperture in front of the lens. The radiation field in a large angular region near the principal direction of the lens can then be determined by Huyghens' principle with a reasonable accuracy from the predicted field in this plane aperture and will be given by a simple Fourier transform of the aperture field. This transform can be evaluated in closed form when the feed pattern belongs to a certain class of patterns. It should be pointed out that the success of using this simpler method for predicting the radiation pattern of the lens depends on how fast the aperture field varies within a wavelength along the aperture. In most practical cases, the field varies slowly enough in the greater part of the aperture to predict the lens radiation field from the aperture field. However, the aperture field will have a discontinuity at the edges of the aperture. The error produced by calculating the radiation pattern from the aperture field is of course larger the stronger the edge discontinuity is. The error can therefore be expected to decrease when the directivity of the feed is increased. However, Jasik has shown[3] that for a 2.5-wavelengths-diameter Luneburg lens, even with an omnidirectional feed which produces an integrable singularity at the edges of the plane aperture, the level of the first side lobe computed by this

method is only about 1 db different from the value that would be found by using the method of expansion of fields in cylindrical wave functions. Although the error may be expected to increase for increasing lens size because of the increasing importance of diffraction effects, it can still be expected that the lens radiation pattern can be predicted from the geometrical optics aperture field with an accuracy that is sufficient for most practical purposes.

For calculating the lens radiation field from the field in a plane aperture in front of the lens, we shall, using geometrical optics, derive the relationship between the aperture field and the feed pattern. Figure 6 shows the circularly symmetric lens and the symbols used in the succeeding calculations.

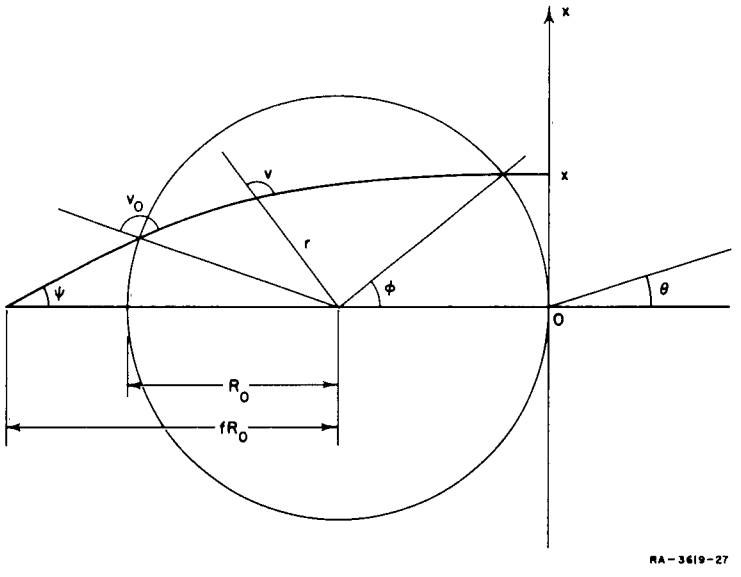

FIG. 6 MODIFIED LUNEBERG LENS AND SYMBOLS USED IN THE DERIVATION OF THE APERTURE FIELD

The equivalent dielectric constant ϵ of the lens depends only upon the radial coordinate. According to Fermat's principle, the path of a ray through the lens is given by

$$\sqrt{\epsilon}\, r \sin v = \text{const.} \qquad (15)$$

where r and v are shown in Fig. 6. The constant is different for different rays. For a ray that starts from the feed and makes an angle of ψ with the principal direction of the lens, this constant has the value

$$\text{const.} = R_o \sin v = R_o f \sin\psi \quad ,$$

where R_o is the radius of the lens. This particular ray will leave the lens at a point on the rim of the lens whose radius vector makes an angle φ with the principal direction of the lens that is therefore given by

$$\sin\varphi = f \sin\psi \quad .$$

If the feed pattern is $g(\psi)$, the amplitude of the field in the plane aperture in front of the lens is proportional to

$$E(\varphi) = \frac{g(\psi)}{\sqrt{\cos\psi}} \quad . \tag{16}$$

Let x be the coordinate along the plane aperture, $x = 0$ being the center of the aperture. The aperture field, expressed in terms of x rather than in terms of ψ, then becomes, using the transformation formula

$$x = R_o \sin\varphi = f R_o \sin\psi \quad ,$$

$$E_a(x) = \frac{g\left[\text{Arc}\sin\left(\frac{x}{fR_o}\right)\right]}{\left[1 - \left(\frac{x}{fR_o}\right)^2\right]^{1/4}} \quad . \tag{17}$$

When we neglect the effect of the spill-over from the feed upon the lens radiation pattern, the lens radiation pattern is now proportional to

$$G(\theta) = \frac{1}{R_o}\int_0^{R_o} E_a(x)\cos(kx\sin\theta)dx$$

$$= \int_0^1 \frac{g\left[\text{Arc}\sin\left(\frac{u}{f}\right)\right]}{\left[1-\left(\frac{u}{f}\right)^2\right]^{1/4}}\cos\left(kR_o\sin\theta u\right)du \quad . \tag{18}$$

This integral shall be evaluated for the following class of feed patterns:

$$g(\psi) = \cos^p\psi \tag{19}$$

where p is an arbitrary positive real number. Many practical feed patterns can be approximated by this type of pattern. With this feed pattern, the radiation pattern of the lens, Eq. (18), can be reduced to

$$G(\theta) = \int_0^1 \left[1-\left(\frac{u}{f}\right)^2\right]^{\frac{p}{2}-\frac{1}{4}}\cos\left(kR_o\sin\theta u\right)du \quad . \tag{20}$$

This integral can be expressed in closed form for $f = 1$, in which case it will be given in terms of a Bessel function of non-integral order. For f different from 1, it does not seem possible to derive a closed-form expression for the lens radiation pattern except when $\frac{p}{2}-\frac{1}{4}$ is an integer, that is when $p = \frac{1}{2}, \frac{5}{2}, \frac{9}{2}, \ldots$. It is interesting to note that for $p = \frac{1}{2}$, the feed produces a uniform illumination of the lens aperture independent of the value of f. The lens radiation pattern in this particular case is

$$G(\theta) = \frac{\sin k R_o \sin\theta}{k R_o \sin\theta} \quad . \tag{21}$$

We want to derive an approximate expression for the lens radiation pattern that is valid for any value of p greater than $\frac{1}{2}$. The fact that f is assumed to be only slightly larger than 1 suggests that a perturbation method be used to derive an approximate closed-form expression for the lens radiation pattern. It would seem natural to expand the integral expression Eq. (20) for $G(\theta)$ in a power series of $(f - 1)$. Unfortunately, Eq. (20), considered as a function of f , cannot be differentiated an arbitrary number of times for $f = 1$. However, when $p > \frac{1}{2}$, the first derivative with respect to f is continuous for $f = 1$. We can therefore use the following approximate expression for $G(\theta)$

$$G(\theta) = \int_0^1 \left(1 - u^2\right)^{\frac{p}{2} - \frac{1}{4}} \cos\left(kR_o \sin\theta u\right) du + (f - 1) \int_0^1 \frac{d}{df}\left[\left(1 - \frac{u^2}{f^2}\right)^{\frac{p}{2} - \frac{1}{4}}\right]_{f = 1} \cos\left(kR_o \sin\theta u\right) du \tag{22}$$

or

$$G(\theta) = \int_0^1 \cos\left(kR_o \sin\theta u\right)\left[\left(1 - u^2\right)^{\frac{p}{2} - \frac{1}{4}} + (f - 1)\left(p - \frac{1}{2}\right)u^2\left(1 - u^2\right)^{\frac{p}{2} - \frac{5}{4}}\right] du \; . \tag{23}$$

When the substitution $u = \cos v$ is introduced in this expression, we find

$$G(\theta) = \left[1 - (f-1)\left|p - \frac{1}{2}\right|\right] \int_0^{\frac{\pi}{2}} \cos(kR_o \sin\theta \cos v) \sin^{p+\frac{1}{2}} v dv$$

$$+ (f-1)\left|p - \frac{1}{2}\right| \int_0^{\frac{\pi}{2}} \cos(kR_o \sin\theta \cos v) \sin^{p-\frac{3}{2}} v dv \quad . \tag{24}$$

The integrals in this equation can be expressed in closed form according to the formula[13]

$$\int_0^{\frac{\pi}{2}} \cos(z \cos v) \sin^{2\nu} v dv = 2^{\nu-1} \Gamma\left(\frac{1}{2}\right) \Gamma\left(\nu + \frac{1}{2}\right) \frac{J_\nu(z)}{z^\nu} \tag{25}$$

where Γ is the gamma function, J the Bessel function, and ν is a number whose real part must exceed $-\frac{1}{2}$.

Finally, we find the following expression on the lens radiation pattern:

$$G(\theta) = \left[1 - (f-1)\left|p - \frac{1}{2}\right|\right] 2^{\frac{p}{2}-\frac{3}{4}} \Gamma\left(\frac{1}{2}\right) \Gamma\left(\frac{p}{2} + \frac{3}{4}\right) \frac{J_{\frac{p}{2}+\frac{1}{4}}(kR_o \sin\theta)}{(kR_o \sin\theta)^{\frac{p}{2}+\frac{1}{4}}}$$

$$+ (f-1)\left|p - \frac{1}{2}\right| 2^{\frac{p}{2}-\frac{7}{4}} \Gamma\left(\frac{1}{2}\right) \Gamma\left(\frac{p}{2} - \frac{1}{4}\right) \frac{J_{\frac{p}{2}-\frac{3}{4}}(kR_o \sin\theta)}{(kR_o \sin\theta)^{\frac{p}{2}-\frac{3}{4}}} \tag{26}$$

We want to normalize this radiation pattern to unity in the principal direction. Since

$$\lim_{z \to 0} \frac{J_\nu(z)}{z^\nu} = \frac{1}{2^\nu \, \Gamma(\nu + 1)} \quad , \tag{27}$$

the normalized radiation pattern is

$$G(\theta) = 2^{\frac{p}{2}+\frac{1}{4}} \frac{\left[1 - (f-1)\left(p - \frac{1}{2}\right)\right] \Gamma\left(\frac{p}{2}+\frac{3}{4}\right) \frac{J_{\frac{p}{2}+\frac{1}{4}}(kR_o \sin\theta)}{(kR_o \sin\theta)^{\frac{p}{2}+\frac{1}{4}}}}{\left[1 - (f-1)\left(p - \frac{1}{2}\right)\right] \frac{\Gamma\left(\frac{p}{2}+\frac{3}{4}\right)}{\Gamma\left(\frac{p}{2}+\frac{5}{4}\right)} + (f-1)\left(p - \frac{1}{2}\right) \frac{\Gamma\left(\frac{p}{2}-\frac{1}{4}\right)}{\Gamma\left(\frac{p}{2}+\frac{1}{4}\right)}}$$

$$+ 2^{\frac{p}{2}+\frac{1}{4}} \frac{\frac{1}{2}(f-1)\left(p - \frac{1}{2}\right) \Gamma\left(\frac{p}{2}-\frac{1}{4}\right) \frac{J_{\frac{p}{2}-\frac{3}{4}}(kR_o \sin\theta)}{(kR_o \sin\theta)^{\frac{p}{2}-\frac{3}{4}}}}{\left[1 - (f-1)\left(p - \frac{1}{2}\right)\right] \frac{\Gamma\left(\frac{p}{2}+\frac{3}{4}\right)}{\Gamma\left(\frac{p}{2}+\frac{5}{4}\right)} + (f-1)\left(p - \frac{1}{2}\right) \frac{\Gamma\left(\frac{p}{2}-\frac{1}{4}\right)}{\Gamma\left(\frac{p}{2}+\frac{1}{4}\right)}} \quad . \tag{28}$$

As already mentioned, this expression is an approximate expression that is valid for $p \geq \frac{1}{2}$. For $p = \frac{1}{2}$, it reduces to

$$G(\theta) = \sqrt{2}\,\Gamma\left(\frac{3}{2}\right) \frac{J_{\frac{1}{2}}(kR_o \sin\theta)}{\sqrt{kR_o \sin\theta}} = \frac{\sin(kR_o \sin\theta)}{(kR_o \sin\theta)} \tag{29}$$

which agrees with the exact expression Eq. (21).

Using existing tables of the Bessel function, the radiation pattern Eq. (28) can be evaluated numerically for integral and half-integral values of p . For practical purposes it should be sufficient to evaluate the radiation pattern for integral values of p . Radiation

patterns for p = 4, 3, and 2 and 1 are shown in Figs. 7-10 as a function of $kR_o \sin\theta$ for f = 1.0 , 1.1, 1.2 and 1.3. Only the main lobe and the first side lobe are shown in these figures. The first side lobe is stronger than all other side lobes, and thus determines the over-all side-lobe level. As expected, the patterns in these figures show that the side-lobe level decreases when p increases (that is, when the feed is made more directive), and it increases when f increases (that is, when the feed is moved further away from the lens). In the limit of very large values of f , the radiation pattern approaches that of a uniformly illuminated aperture, so that the side-lobe level approaches -13.2 db. As mentioned previously, the effect of the spill-over from the feed has not been taken into account.

Equation (28) for the lens radiation pattern is only applicable for $p \geq \frac{1}{2}$. Since the case of an omnidirectional feed (p = 0) will be of particular interest in the testing of the experimental lens, we shall consider the case p = 0 separately. For p = 0 , Eq. (20) reduces to

$$G(\theta) = \int_0^1 \left[1 - \left(\frac{u}{f}\right)^2\right]^{-\frac{1}{4}} \cos(kR_o \sin\theta u)\, du \quad , \tag{30}$$

which, except for a constant multiplier, using Eq. (25), can be written

$$G(\theta) = \int_{\text{Arc}\cos\left(\frac{1}{f}\right)}^{\frac{\pi}{2}} \cos(kfR_o \sin\theta \cos v) \sin^{\frac{1}{2}} v\, dv$$

$$= 2^{-\frac{3}{4}} \Gamma\left(\frac{1}{2}\right) \Gamma\left(\frac{3}{4}\right) \frac{J_{\frac{1}{4}}(kfR_o \sin\theta)}{(kR_o \sin\theta)^{\frac{1}{4}}} - I \quad , \tag{31}$$

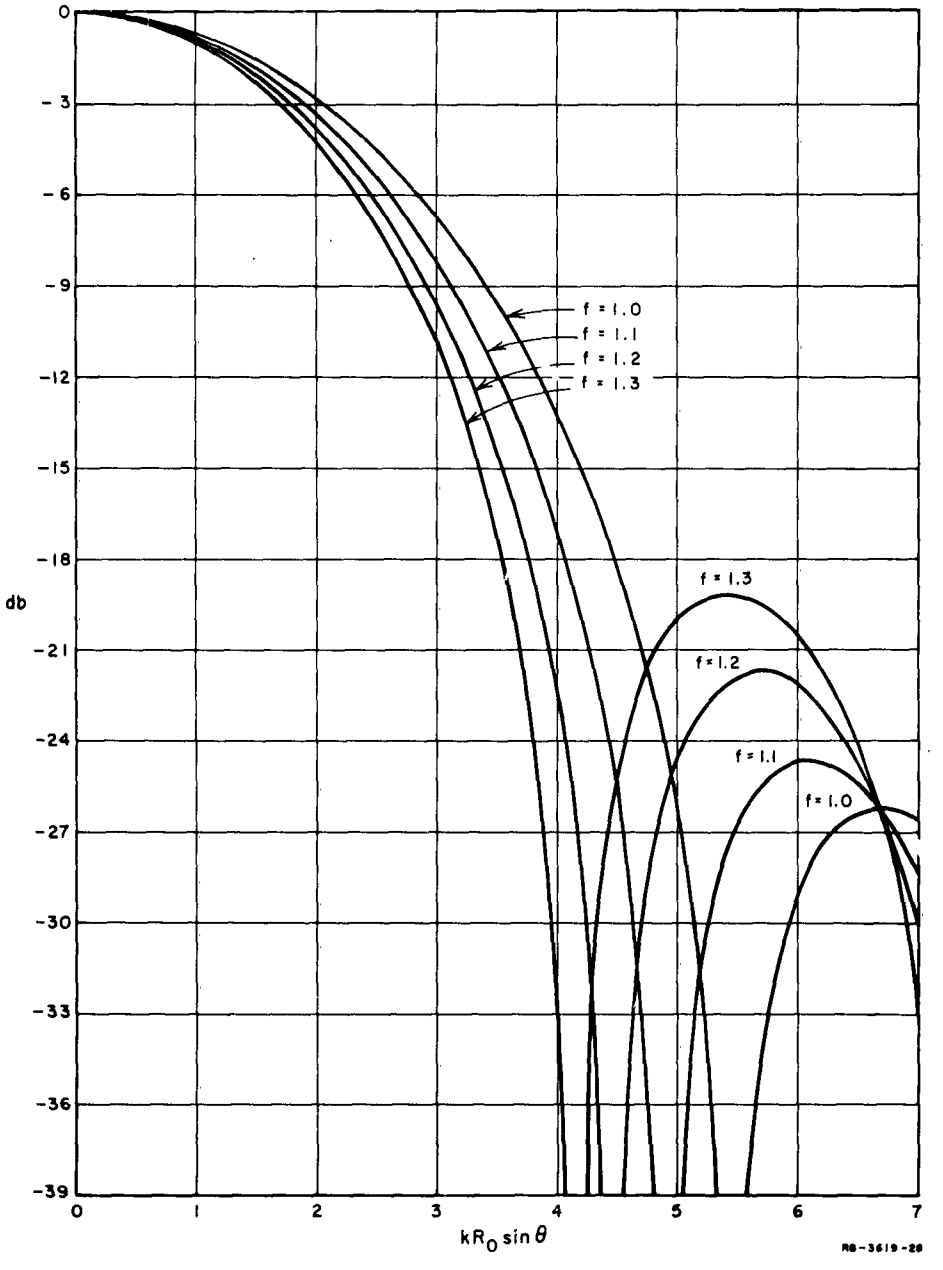

FIG. 7 THEORETICAL RADIATION PATTERN OF MODIFIED LUNEBURG LENS WITH $\cos^4 \psi$ PATTERN OF THE FEED (p = 4)

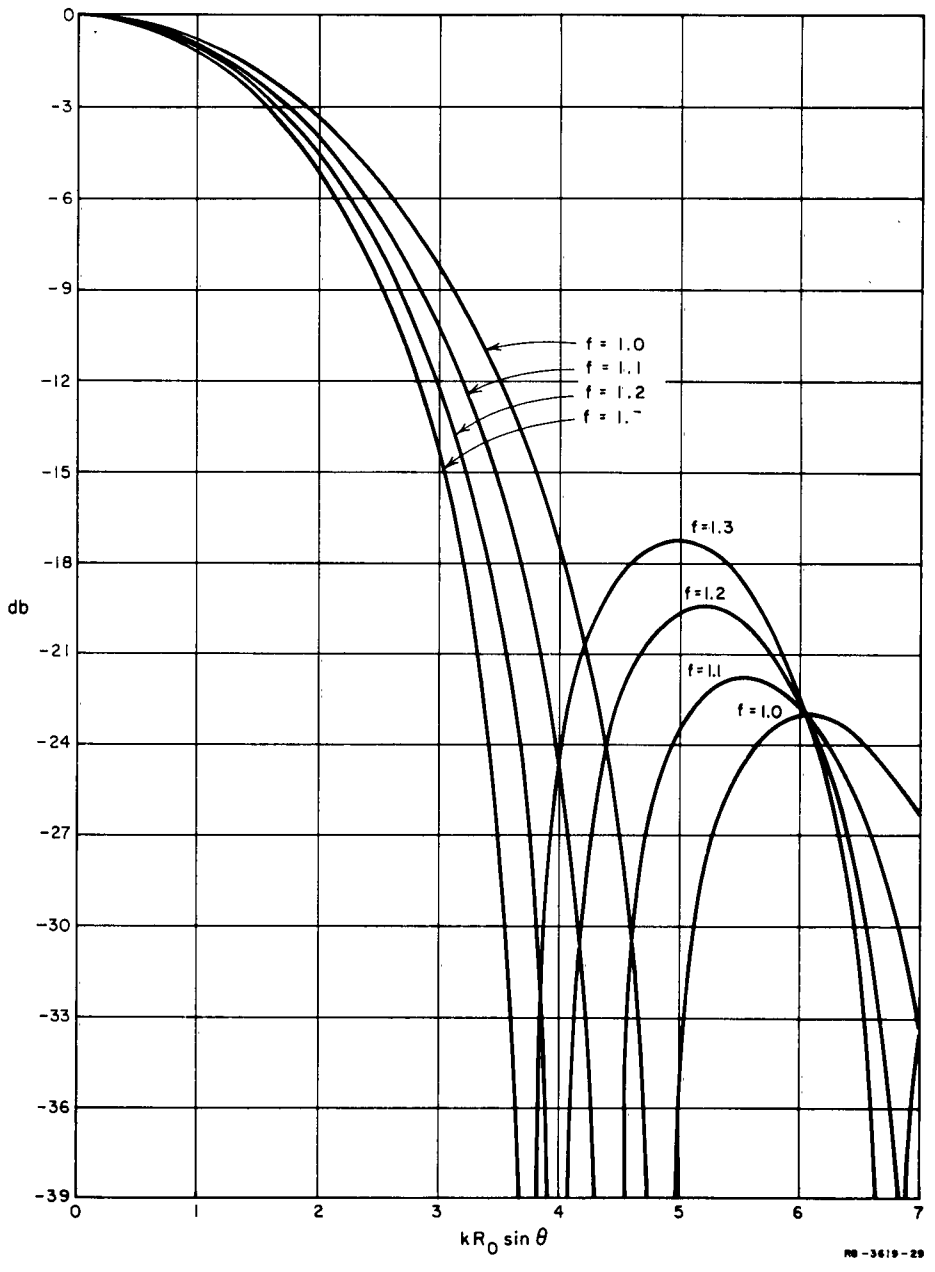

FIG. 8 THEORETICAL RADIATION PATTERN OF MODIFIED LUNEBERG LENS WITH $\cos^3 \psi$ PATTERN OF THE FEED ($p = 3$)

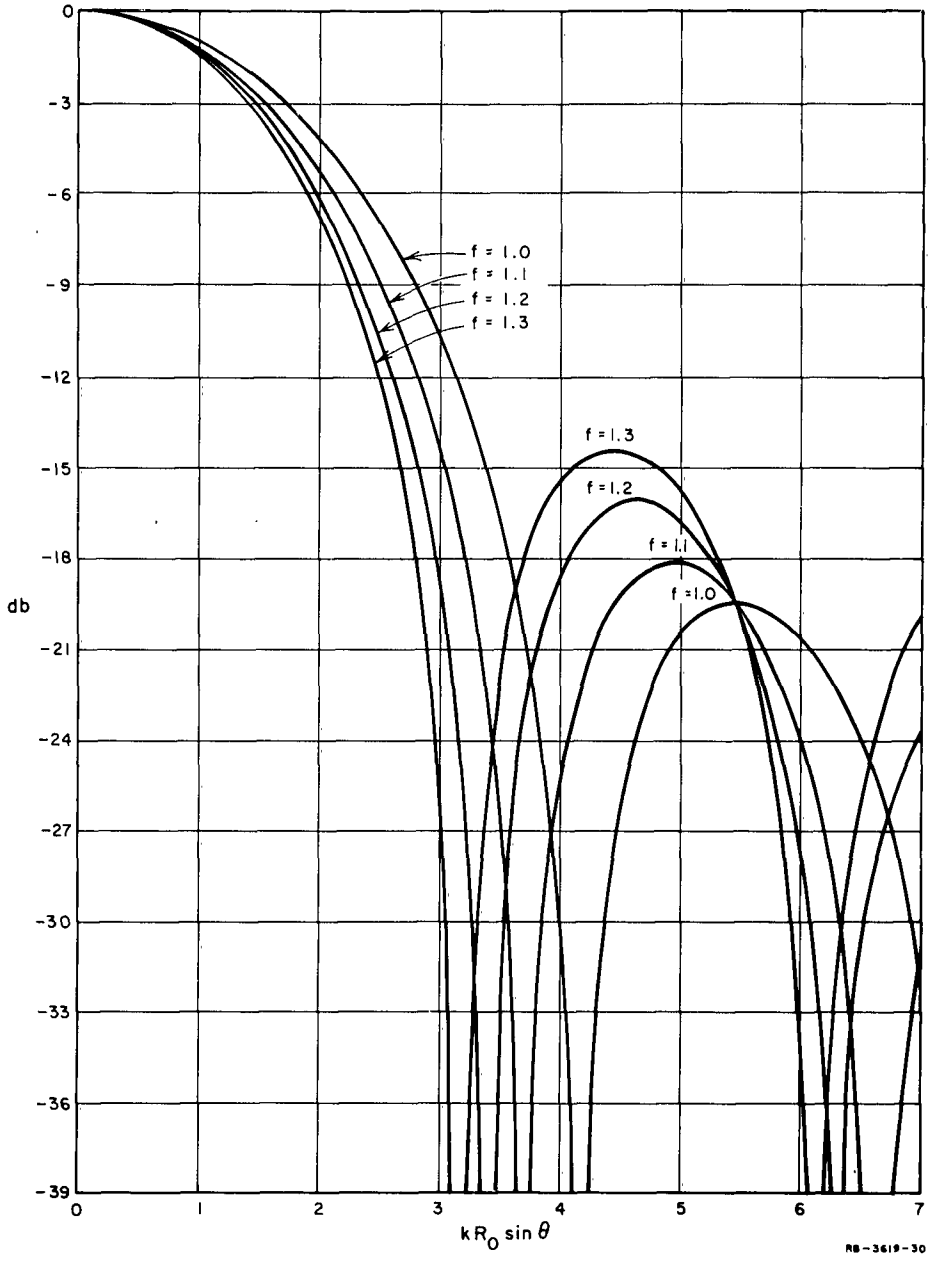

FIG. 9 THEORETICAL RADIATION PATTERN OF MODIFIED LUNEBURG LENS WITH $\cos^2 \psi$ PATTERN OF THE FEED (p = 2)

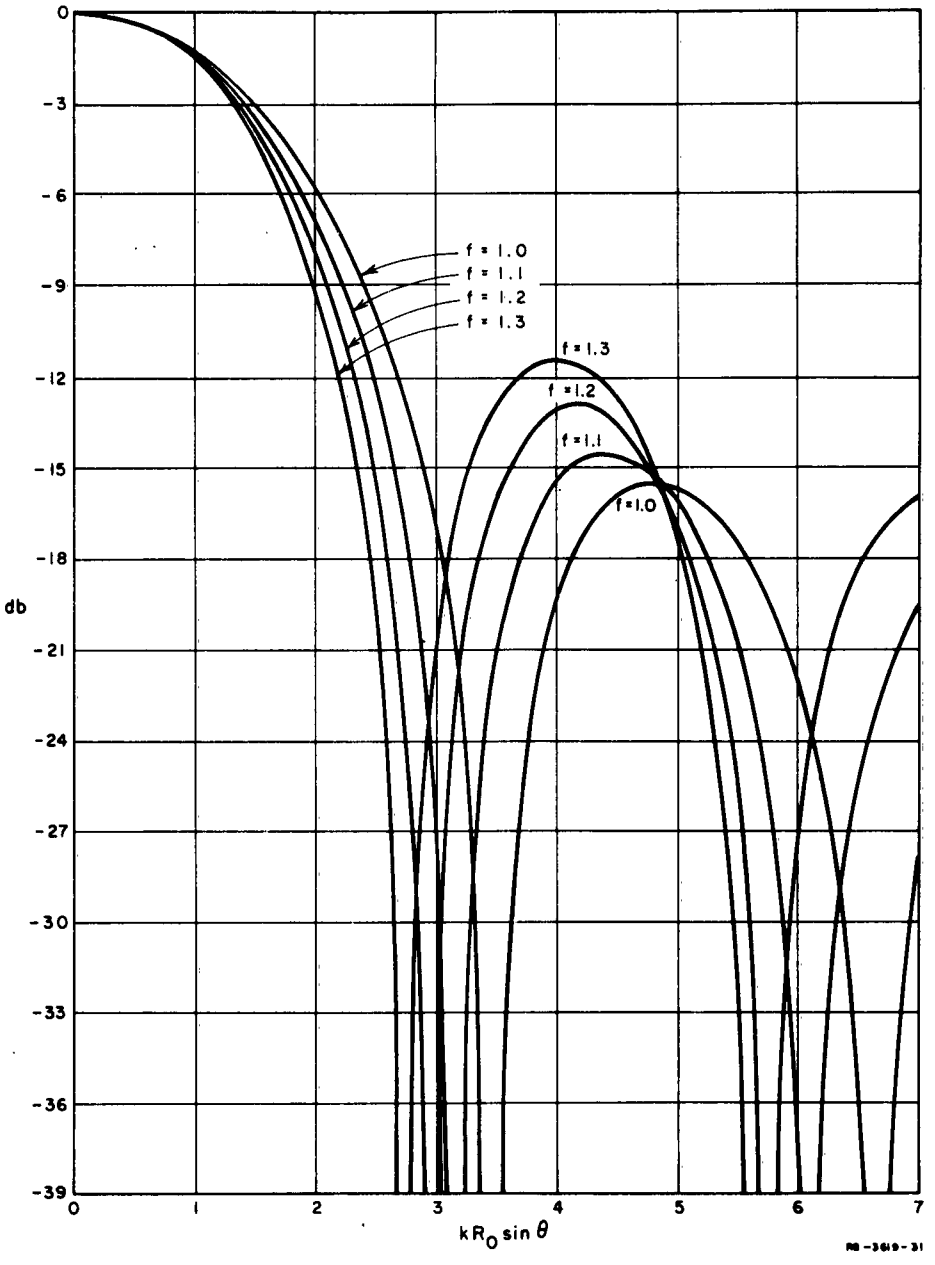

FIG. 10 THEORETICAL RADIATION PATTERN OF MODIFIED LUNEBURG LENS WITH $\cos \psi$ PATTERN OF THE FEED ($p = 1$)

where

$$I = \int_0^{\text{Arc}\cos\left(\frac{1}{f}\right)} \cos\left(kfR_o \sin\theta \cos v\right) \sin^{\frac{1}{2}} v\, dv \quad . \tag{32}$$

When f is only slightly larger than 1, and when we consider only the radiation pattern including the first side lobes, it is permissible in the expression for I to introduce the following approximations

$$\cos\left(kfR_o \sin\theta \cos v\right) \approx \cos\left(kfR_o \sin\theta\right) + \frac{1}{2} kfR_o \sin\theta \sin\left(kfR_o \sin\theta\right)\, v^2$$

$$\sin^{\frac{1}{2}} v \approx v^{\frac{1}{2}}$$

$$\text{Arc}\cos\frac{1}{f} \approx \sqrt{2\left(1 - \frac{1}{f}\right)} \quad .$$

When these approximations are introduced in Eq. (32), and Eq. (32) is introduced in Eq. (31), we find the following approximate expression for the normalized lens radiation pattern

$$G(\theta) = \frac{\left\{ 2^{-\frac{3}{4}} \Gamma\left(\frac{1}{2}\right) \Gamma\left(\frac{3}{4}\right) \frac{J_{\frac{1}{4}}\left(kfR_o \sin\theta\right)}{\left(kfR_o \sin\theta\right)^{\frac{1}{4}}} \right\} - \frac{2}{3}\left[\frac{2(f-1)}{f}\right]^{\frac{3}{4}} \left[\cos\left(kfR_o \sin\theta\right) + \frac{3}{7}\frac{f-1}{f} kfR_o \sin\theta \sin\left(kfR_o \sin\theta\right)\right]}{\frac{1}{2}\Gamma\left(\frac{1}{2}\right)\frac{\Gamma\left(\frac{3}{4}\right)}{\Gamma\left(\frac{5}{4}\right)} - \frac{2}{3}\left[\frac{2(f-1)}{f}\right]^{\frac{3}{4}}} \tag{33}$$

For $f = 1$, this expression reduces to the result found by Jasik.[3] The radiation pattern Eq. (33) is plotted in Fig. 11 for $f = 1.0$, 1.1 and 1.2. The pattern for $f = 1.3$ is very close to that for $f = 1.2$ and has not been plotted. In contrast to what was found for $p = 1,2,3$ and 4, the side-lobe level is seen for $p = 0$ to decrease for increasing values of $\underline{f}$, approaching -13.2 db for large values of $\underline{f}$.

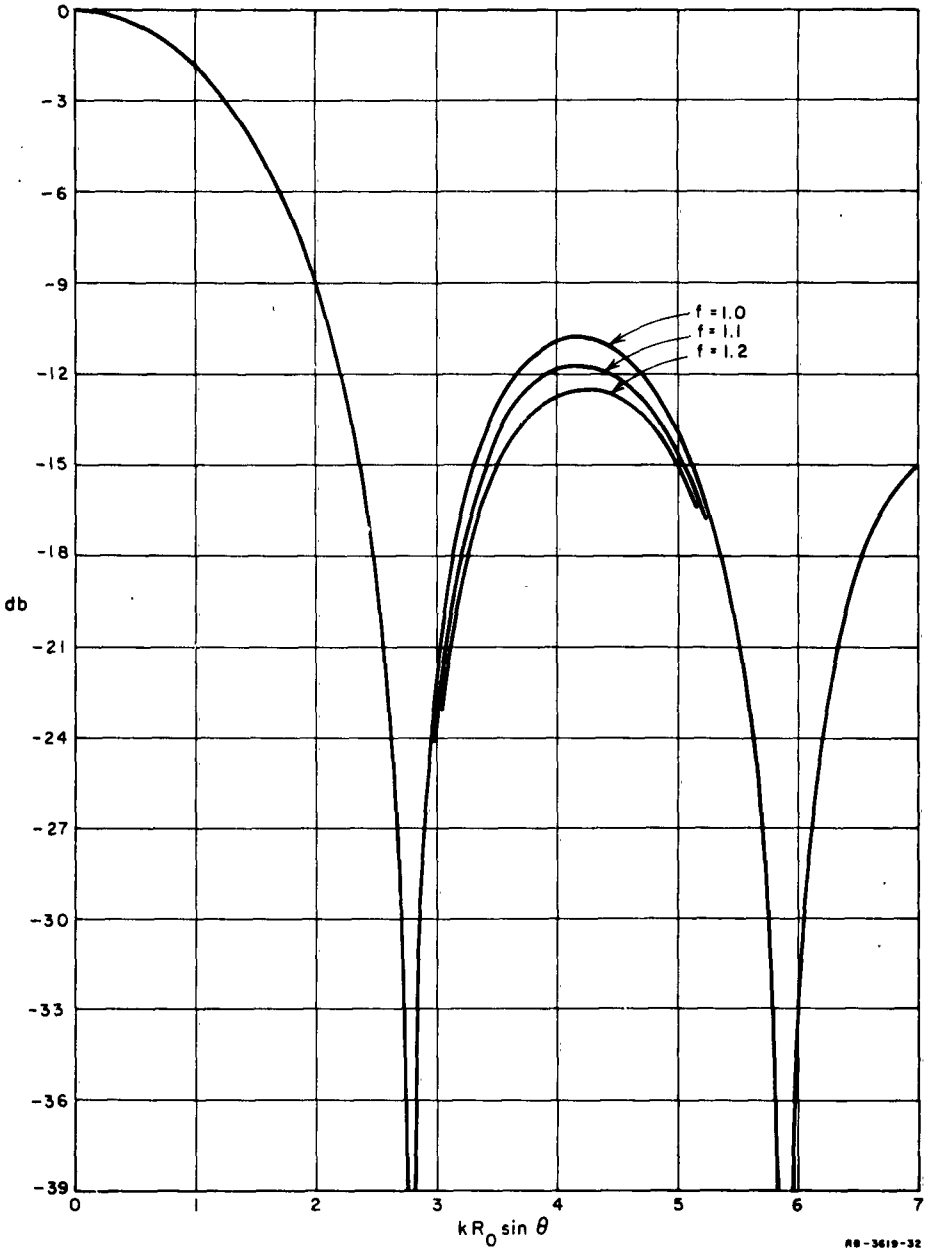

FIG. 11 THEORETICAL RADIATION PATTERN OF MODIFIED LUNEBURG LENS WITH OMNIDIRECTIONAL PATTERN OF THE FEED (p = 0)

IV MEASURED PERFORMANCE OF EXPERIMENTAL SQUARE-MESH WIRE-GRID LENS ANTENNA

The details of the design and construction of the experimental square-mesh wire-grid modified Luneburg lens antenna were described in Sec. II. In this section, we present the measured performance of the antenna, and compare this with the theoretical performance as determined from the design formulas derived in Sec. III.

According to the design formulas in Sec. II, the experimental lens antenna is to be fed by a source whose phase center is located at a distance from the center of the lens corresponding to f = 1.18. For most of the radiation patterns to be presented here, the feed antenna was moved back and forth in the radial direction of the lens to find the optimum feed position, that is, the feed position which results in the deepest first minima of the far-zone radiation pattern. The measured optimum values of f were found to be between 1.14 and 1.27, which is fairly close to the theoretical value f = 1.18. The optimum feed position was found to be rather uncritical, and the lens would in most cases operate satisfactorily for f = 1.18.

The primary purpose of the radiation pattern measurements was to test the proper functioning of the lens itself. For this reason, only azimuth patterns of the lens antenna were measured, since the vertical patterns are rather broad and are essentially determined by the flare angle and the aperture height of the radial horn. The vertical patterns will have a maximum at an elevation angle (the angle between the field direction and the ground plane) of about 15 degrees. The relative azimuth patterns are practically the same for elevation angles up to about 15 degrees, and were all measured at an elevation angle of 7 degrees.

Regardless of the type of feed used, the proper functioning of the lens can be told from the radiation pattern of the lens antenna in the immediate neighborhood of the main beam. The following two criteria were used to determine whether the lens was functioning properly:

(1) The forming of a main beam with deep first nulls will indicate that the phase of the field in the plane aperture in front of the lens is nearly constant, as expected.

(2) When the beamwidth and the level of the first side lobes are close to the theoretically predicted values, the amplitude distribution of the field across the plane aperture in front of the lens is also as expected.

Since the main purpose of the measurements was to test whether the above conditions were satisfied for the experimental lens, the choice of which type of a feed should be used for testing the lens was not very critical. Two very simple types of feed antennas were used for testing the lens: a quarter-wave dipole, and a simple Yagi antenna. The quarter-wave dipole was mounted on the ground plane of the radial horn and fed from beneath the ground plane. The free-space azimuth radiation pattern of this dipole is omnidirectional. Although the azimuth pattern of the dipole will no longer be omnidirectional when the dipole is placed in the horn, it will with a fair approximation be so.

The directional Yagi antenna consisted of one driven quarter-wave element, one reflector element, and six director elements, all mounted on the ground plane of the radial horn. The measured free-space azimuth radiation pattern of the experimental Yagi antenna feed is shown as the solid curve in Fig. 12. The dotted curve in this figure is the cosine-squared pattern, which approximates the measured pattern fairly well in a large angular region near the principal direction of the feed. When the Yagi antenna is placed on the ground plane of the radial horn, the azimuth pattern of the feed can still be expected to be close to the measured pattern shown in Fig. 12. The phase center of the Yagi antenna was taken to be the position of the driven element, since the Yagi antenna can be considered to be a tapered surface-wave antenna with quasi-spherical wave fronts emerging from the driven element.

The above two types of feed antenna were not very broadband. Feed antennas were therefore constructed for each frequency at which the lens was tested.

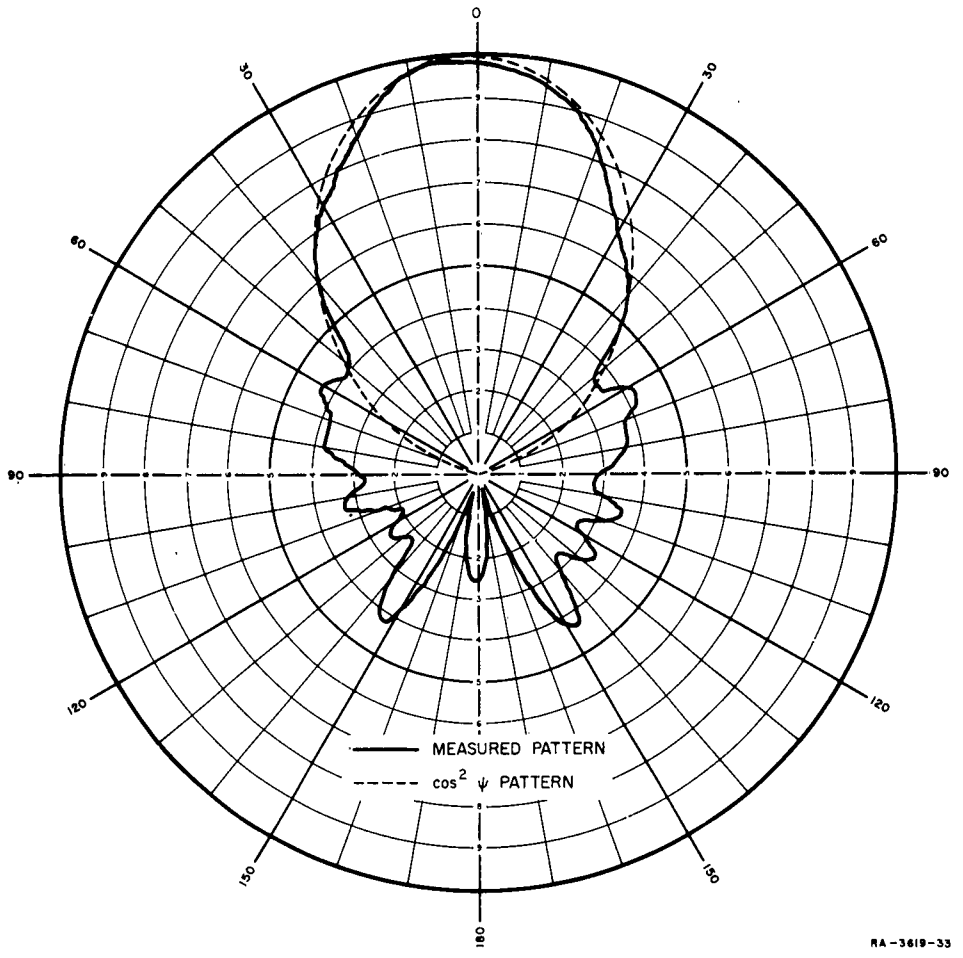

FIG. 12 FREE-SPACE AMPLITUDE RADIATION PATTERN OF YAGI ANTENNA USED TO TEST THE EXPERIMENTAL LENS ANTENNA

According to the design formulas developed in Sec. II, the experimental lens antenna should operate satisfactorily roughly in the frequency band 750 Mc-1700 Mc. The measured lens radiation patterns verified this.

With the dipole-type feed, the lens antenna was tested at 750 Mc, 1000 Mc, 1250 Mc, and 1500 Mc. The measured azimuth radiation patterns of the lens antenna are shown in Figs. 13-19. Most of the measured patterns (shown as the solid curves in these figures) compare reasonably well with the theoretical patterns (shown as dotted curves). The

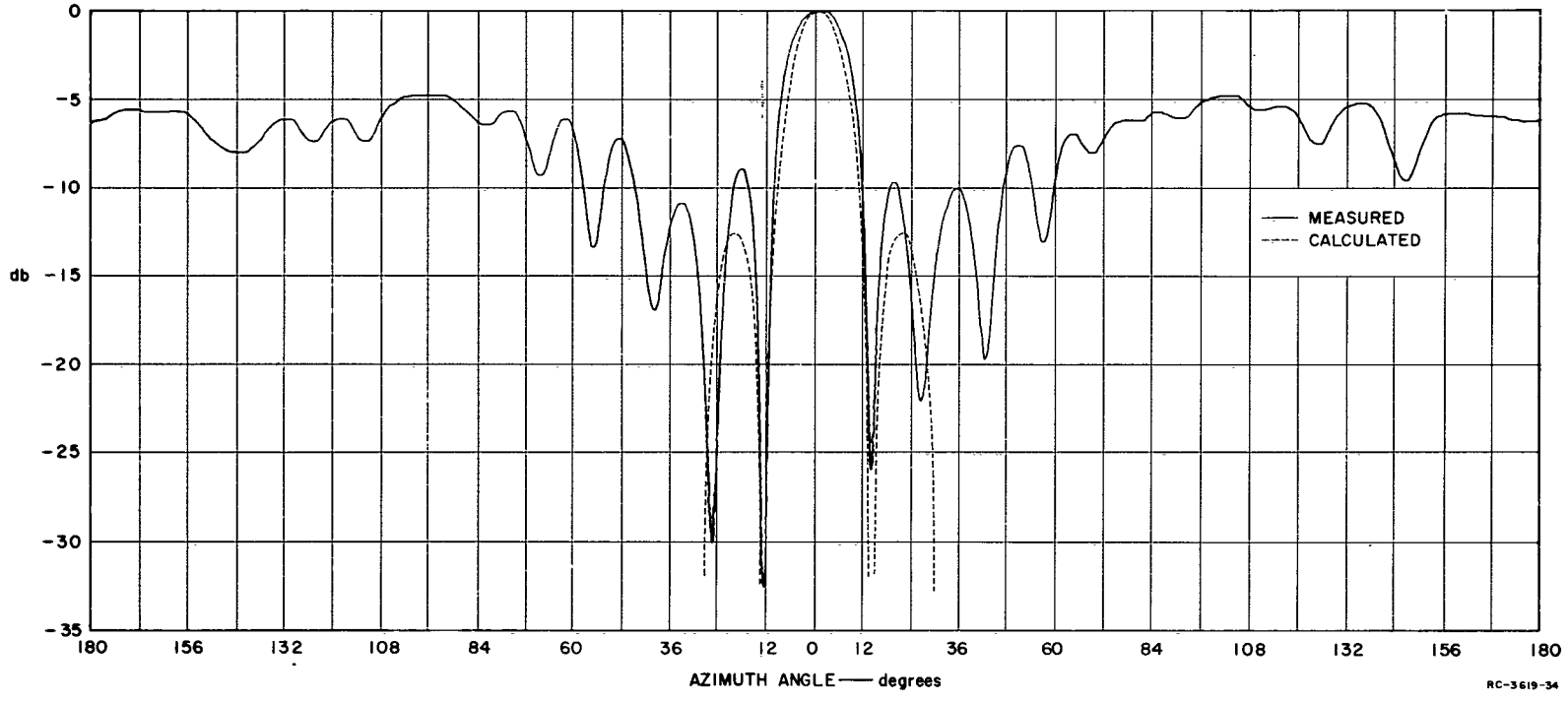

FIG. 13 AZIMUTH RADIATION PATTERN OF EXPERIMENTAL LENS ANTENNA WITH OMNIDIRECTIONAL FEED—PRINCIPAL DIRECTION DIAGONAL TO GRID WIRES, f = 1.14, ELEVATION ANGLE = 7°, FREQUENCY = 750 Mc

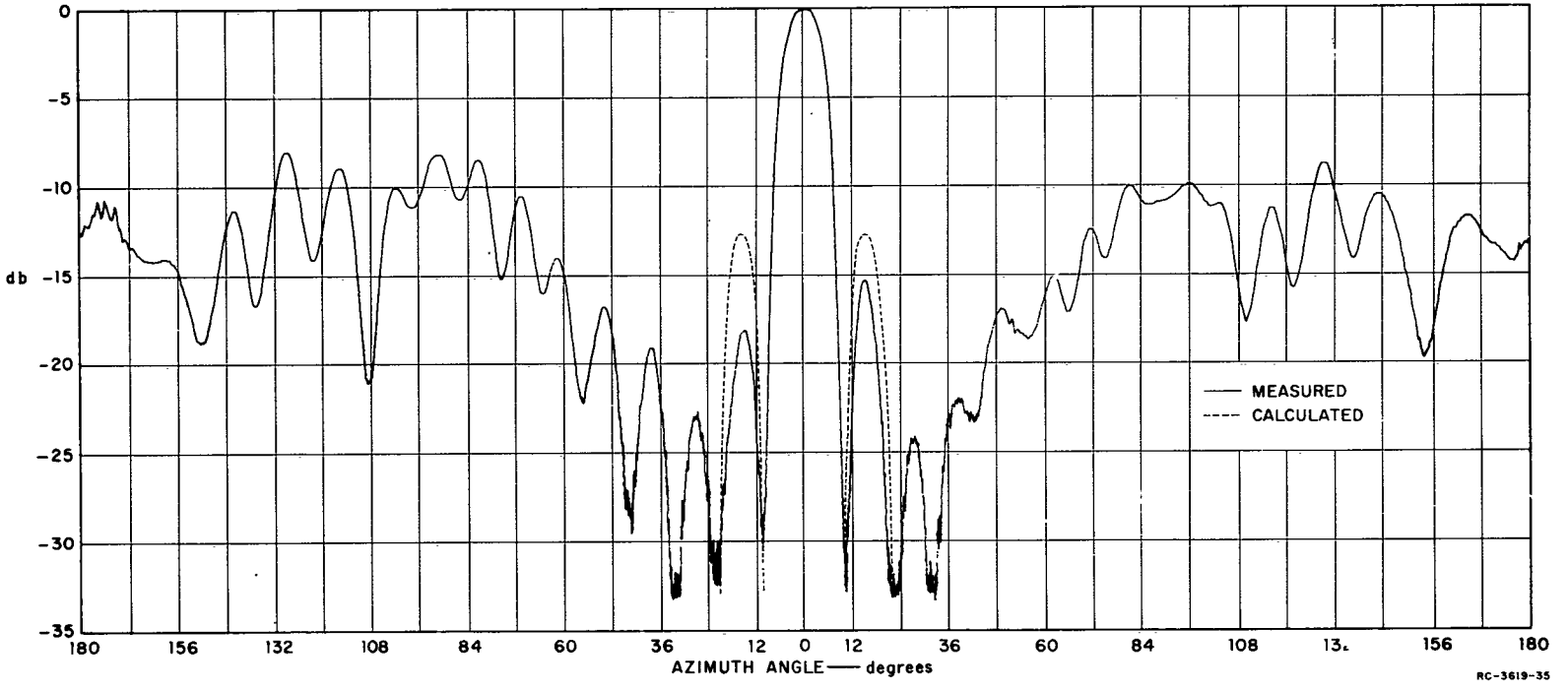

FIG. 14 AZIMUTH RADIATION PATTERN OF EXPERIMENTAL LENS ANTENNA WITH OMNIDIRECTIONAL FEED–PRINCIPAL DIRECTION DIAGONAL TO GRID WIRES, f = 1.20, ELEVATION ANGLE = 7°, FREQUENCY = 1000 Mc

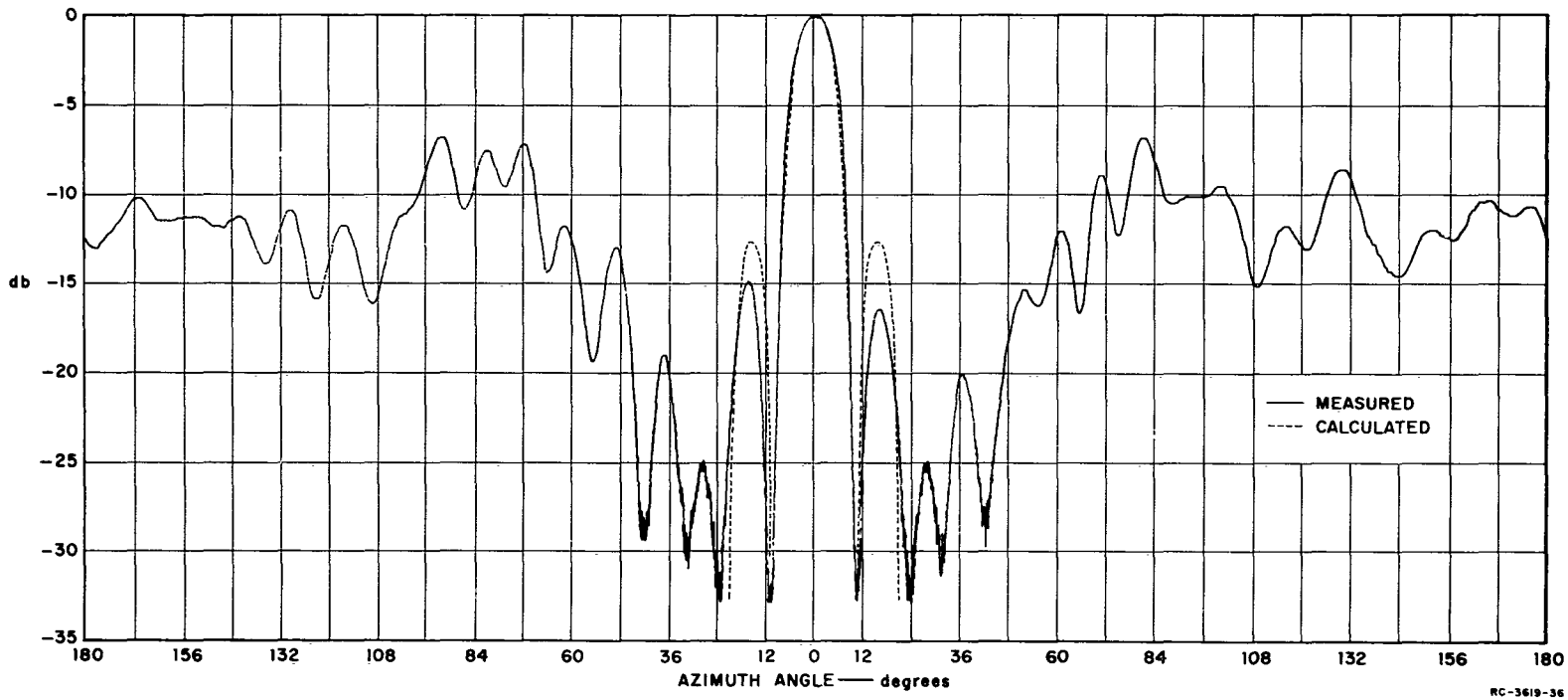

FIG. 15 AZIMUTH RADIATION PATTERN OF EXPERIMENTAL LENS ANTENNA WITH OMNIDIRECTIONAL FEED–PRINCIPAL DIRECTION PARALLEL TO GRID WIRES, f = 1.20, ELEVATION ANGLE = 7°, FREQUENCY = 1000 Mc

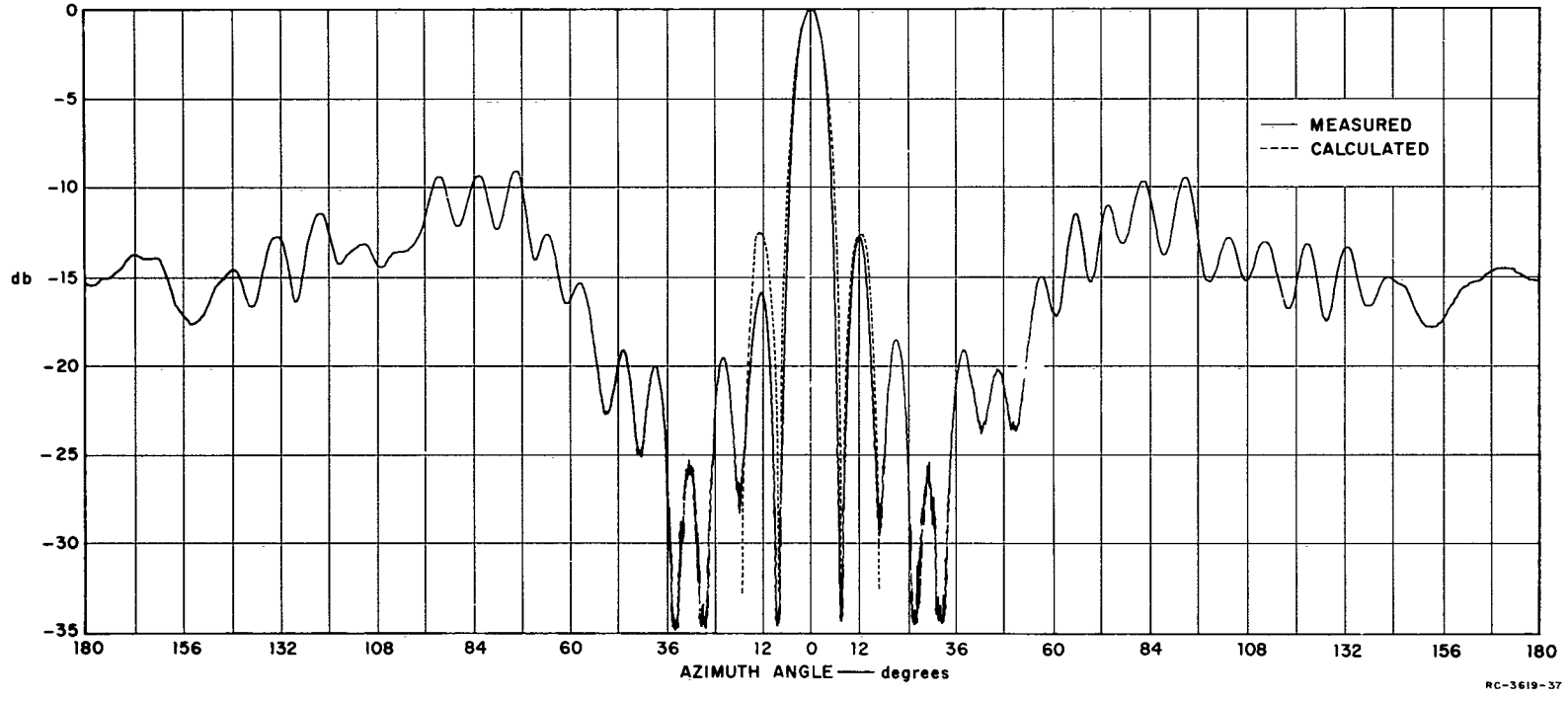

FIG. 16 AZIMUTH RADIATION PATTERN OF EXPERIMENTAL LENS ANTENNA WITH OMNIDIRECTIONAL FEED–PRINCIPAL DIRECTION DIAGONAL TO GRID WIRES, f = 1.17, ELEVATION ANGLE = 7°, FREQUENCY = 1250 Mc

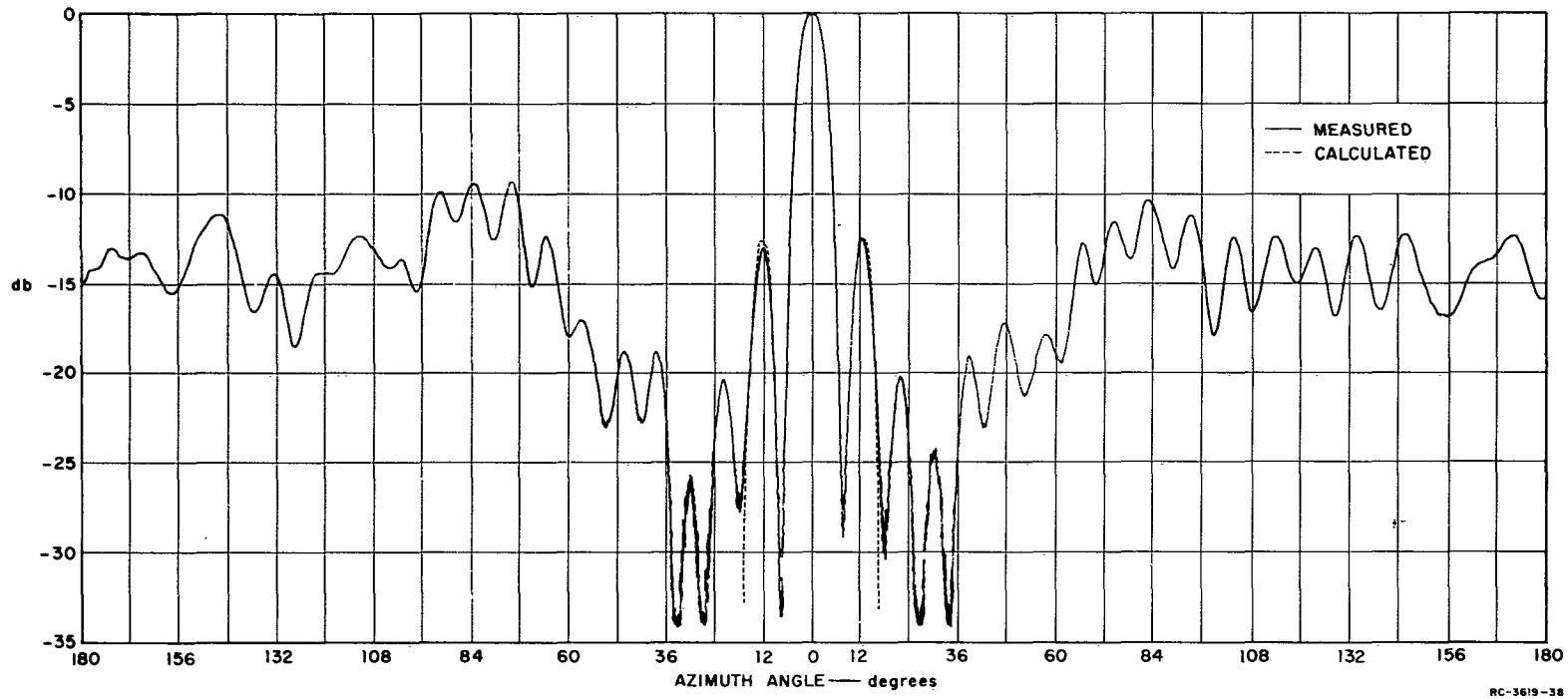

FIG. 17 AZIMUTH RADIATION PATTERN OF EXPERIMENTAL LENS ANTENNA WITH OMNIDIRECTIONAL FEED–PRINCIPAL DIRECTION PARALLEL TO GRID WIRES, f = 1.17, ELEVATION ANGLE = 7°, FREQUENCY = 1250 Mc

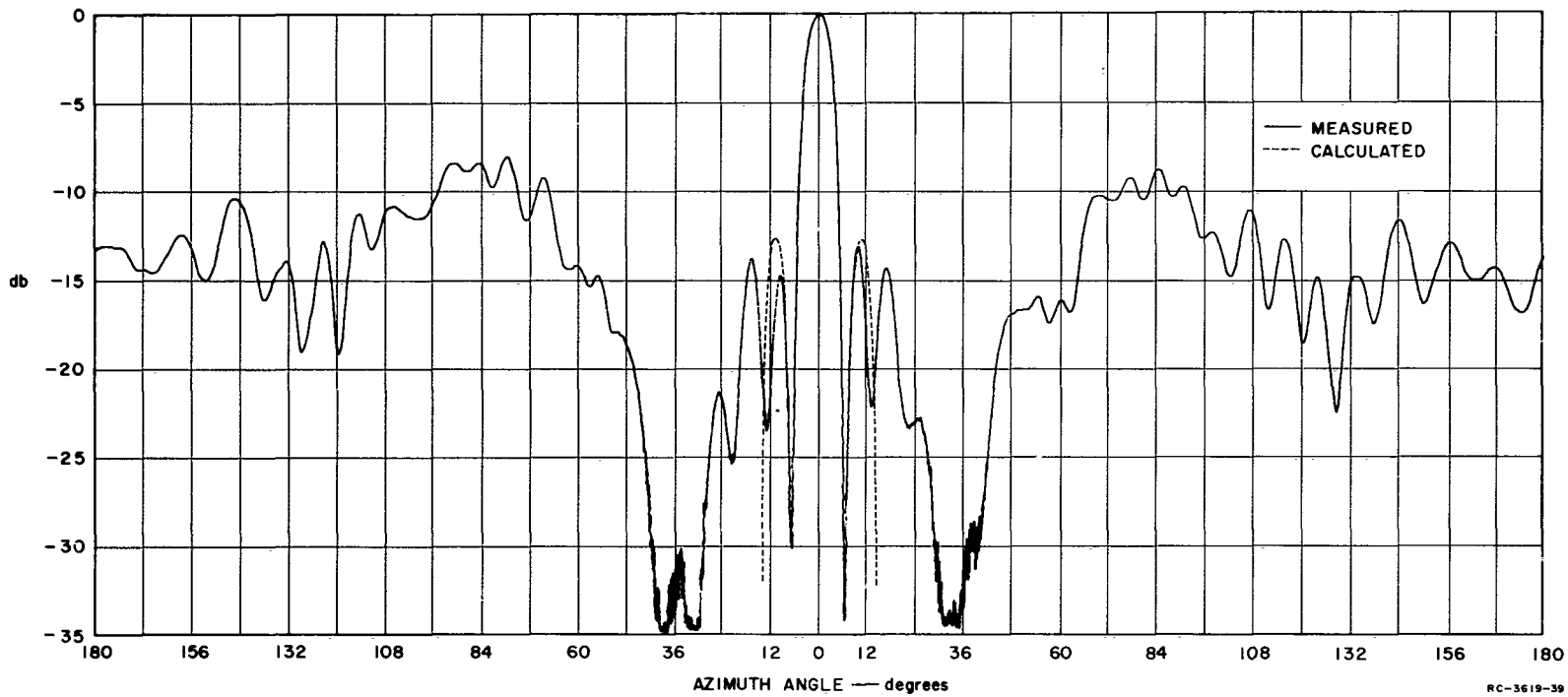

FIG. 18 AZIMUTH RADIATION PATTERN OF EXPERIMENTAL LENS ANTENNA WITH OMNIDIRECTIONAL FEED–PRINCIPAL DIRECTION DIAGONAL TO GRID WIRES, f = 1.14, ELEVATION ANGLE = 7°, FREQUENCY = 1500 Mc

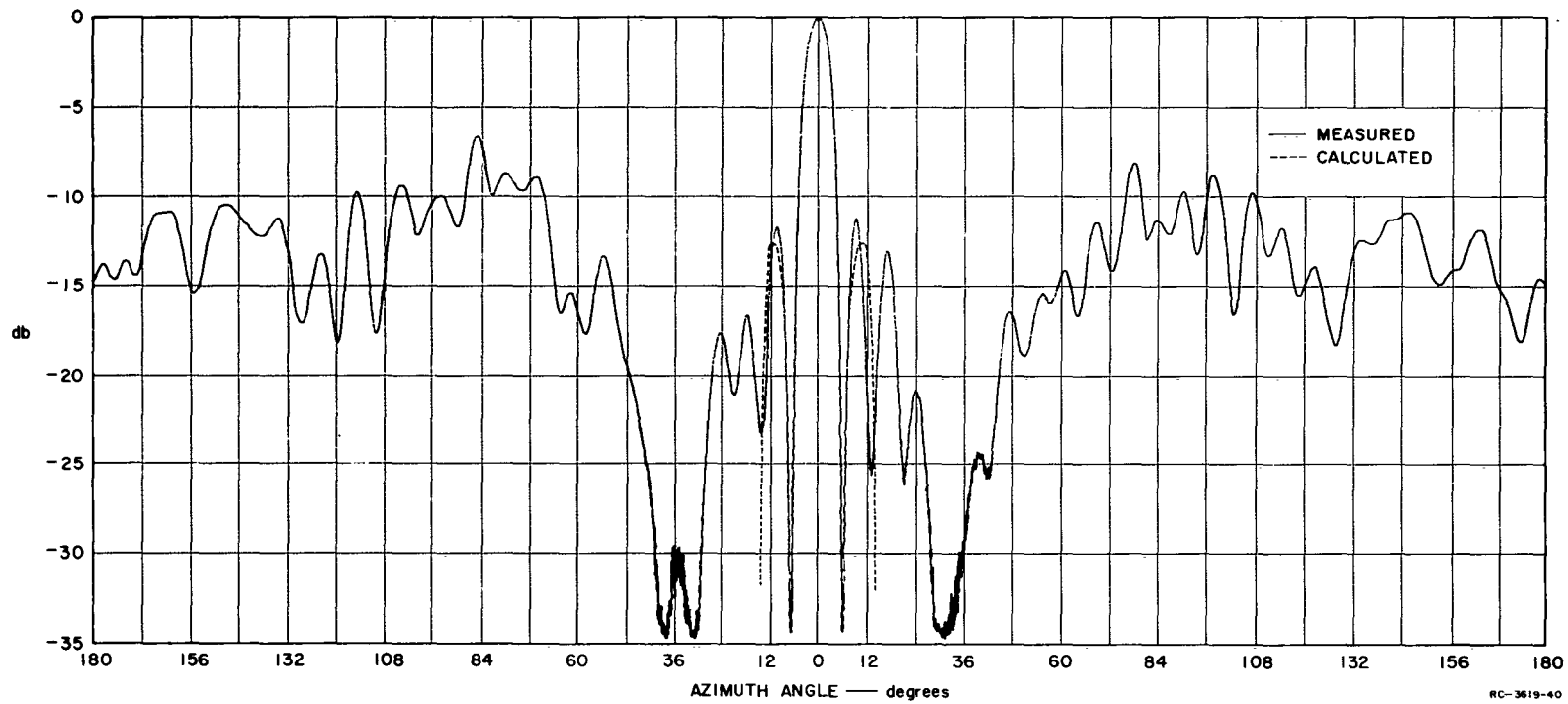

FIG. 19 AZIMUTH RADIATION PATTERN OF EXPERIMENTAL LENS ANTENNA WITH OMNIDIRECTIONAL FEED–PRINCIPAL DIRECTION PARALLEL TO GRID WIRES, f = 1.14, ELEVATION ANGLE = 7°, FREQUENCY = 1500 Mc

theoretical patterns were calculated from the design formulas developed in Sec. III with p = 0 and f = 1.20. At 750 Mc, the level of the first side lobe of the measured lens radiation pattern is somewhat higher than the expected -12.4 db. The reason for this discrepancy is presumed to be that, at 750 Mc, the height of the horn aperture is only one wavelength so that diffraction effects at the back edge of the horn can become significant.

The measured lens radiation patterns shown in Figs. 13-19 very clearly exhibit the formation of a main beam with first nulls more than 25 db deep. The patterns show a slight degree of asymmetry of the lens antenna, the level of the first side lobes on each side of the main beam differing by up to 3 db. The difference between the radiation patterns when the principal direction is diagonal and when it is parallel to the grid wires is relatively small. Anisotropy effects are therefore negligible in the tested frequency band. It is seen that the radiation field rises to a fairly constant level in a large angular region away from the principal direction. This level is higher than the level of the first side lobes and is caused by the back radiation of the dipole feed. The shape as well as the level of the radiation pattern in this angular region is not of any importance in evaluating the properties of the lens itself, since the radiation field in this region can always be suppressed by using a suitable directional feed rather than an omnidirectional feed. It can therefore be concluded that the lens functions properly in the frequency band 750 Mc-1500 Mc. For frequencies below 750 Mc, the radiation efficiency of the radial horn drops rapidly, and for frequencies above 1500 Mc, the lens radiation pattern starts to deteriorate. Above 1500 Mc, the first nulls will be filled in, the over-all side-lobe level will rise, and the radiation pattern will vary with the azimuthal position of the feed. Patterns for frequencies up to 2000 Mc were measured with the directional feed and will be shown later.

The purpose of testing the experimental lens antenna with a directional feed was twofold: The first side lobes of the lens radiation pattern are expected to be lower than in the case of an omnidirectional feed. Thus, a comparison between the measured radiation patterns and

the theoretical patterns derived from the design formulas in Sec. III will again demonstrate the usefulness of the formulas. Also, it can be demonstrated that the radiation field in the region outside the region between the first side lobes can be drastically suppressed by using a directional feed, so that the first side lobes will often determine the over-all side-lobe level of the radiation pattern.

The lens antenna with the directional feed was tested at 1250 Mc, 1500 Mc, 1750 Mc, and 2000 Mc. The measured azimuth radiation patterns of the lens antenna are shown in Figs. 20-26. Most of the measured patterns, which are shown as the solid curves in these figures, compare reasonably well with the theoretical patterns, which are shown as the dotted curves. The theoretical patterns were calculated from the design formulas developed in Sec. III with $p = 2$ and $f = 1.20$. The theoretical side-lobe level is -16 db. At 1750 Mc, the pattern whose principal direction is parallel to one set of grid wires (see Fig. 25) has a fairly high first side lobe. The discrepancy between the patterns in Fig. 24 and Fig. 25 can presumably be ascribed to the fact that at around 1750 Mc the grid starts to become notably anisotropic. For frequencies exceeding 1750 Mc, the lens radiation pattern deteriorates rapidly. A single pattern measured at 2000 Mc (Fig. 26) serves to illustrate this.

With a more directional feed, the lens can be operated to a substantially higher frequency, which is limited mainly by the fact that the mesh size of the grid meshes should not exceed about 0.2 wavelength. The ultimate high-frequency limit of the lens is thus about 3000 Mc. The lens was not tested with a more directional feed.

As expected, the lens radiation patterns with the directional feed (Figs. 20-24) exhibit the same essential characteristics near the main beam as the corresponding lens patterns for the omnidirectional feed, except that the main beam is somewhat broader and the level of the first side lobes somewhat lower when the directional feed is used than when the omnidirectional feed is used. Outside the region between the first side lobes of the lens radiation pattern, the directional feed is seen to have the effect of suppressing the radiation field strongly at most

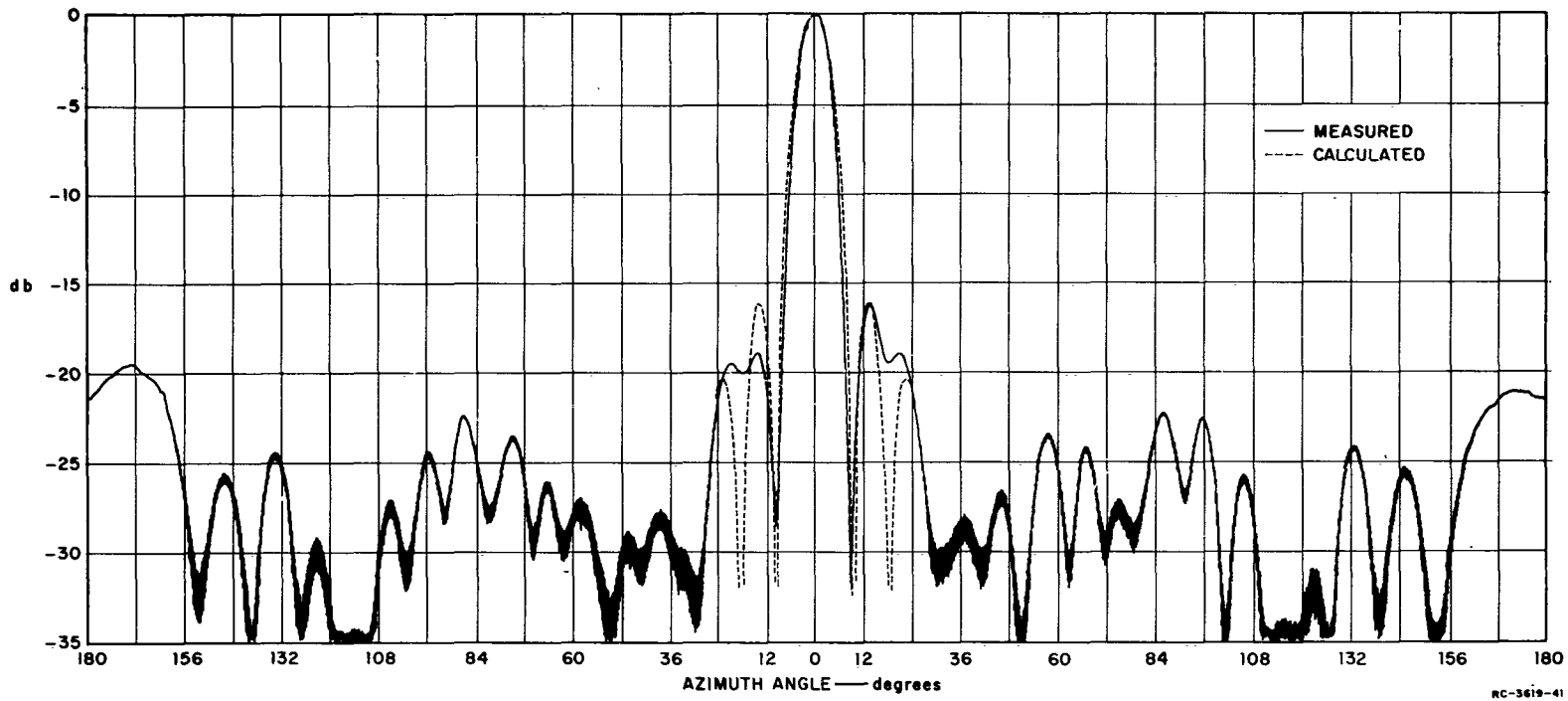

FIG. 20 AZIMUTH RADIATION PATTERN OF EXPERIMENTAL LENS ANTENNA WITH DIRECTIONAL FEED–PRINCIPAL DIRECTION DIAGONAL TO GRID WIRES, f = 1.23, ELEVATION ANGLE = 7°, FREQUENCY = 1250 Mc

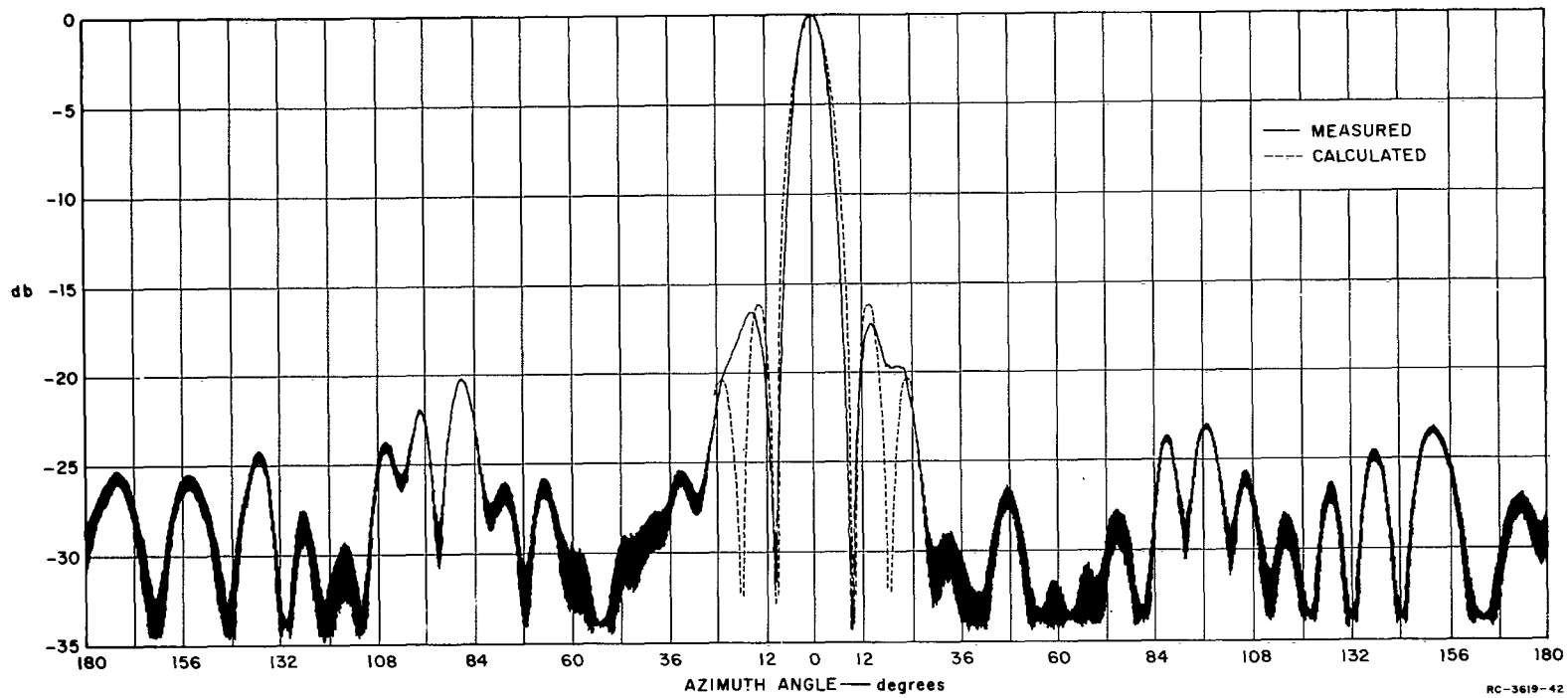

FIG. 21 AZIMUTH RADIATION PATTERN OF EXPERIMENTAL LENS ANTENNA WITH DIRECTIONAL FEED–PRINCIPAL DIRECTION PARALLEL TO GRID WIRES, f = 1.20, ELEVATION ANGLE = 7°, FREQUENCY = 1250 Mc

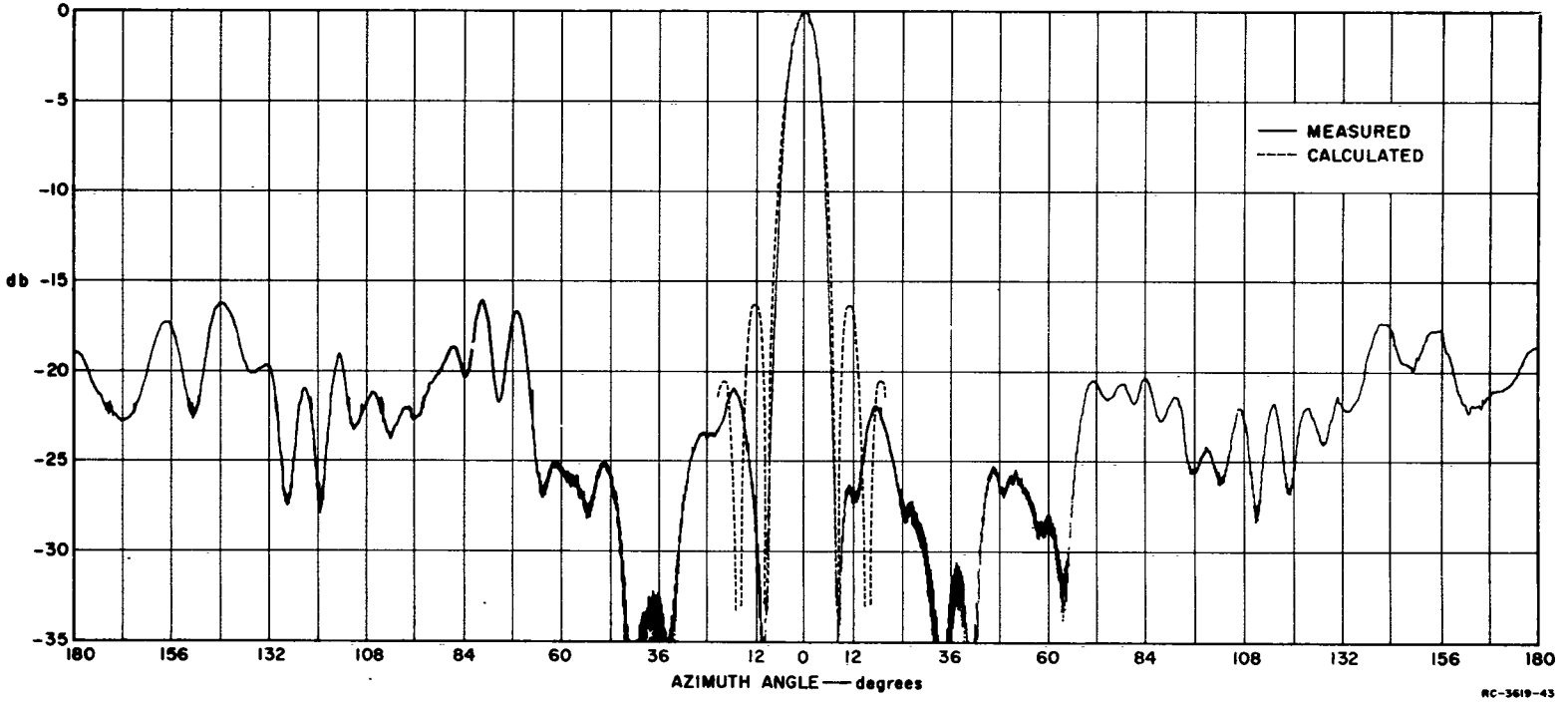

FIG. 22 AZIMUTH RADIATION PATTERN OF EXPERIMENTAL LENS ANTENNA WITH DIRECTIONAL FEED–PRINCIPAL DIRECTION DIAGONAL TO GRID WIRES, f = 1.23, ELEVATION ANGLE = 7°, FREQUENCY = 1500 Mc

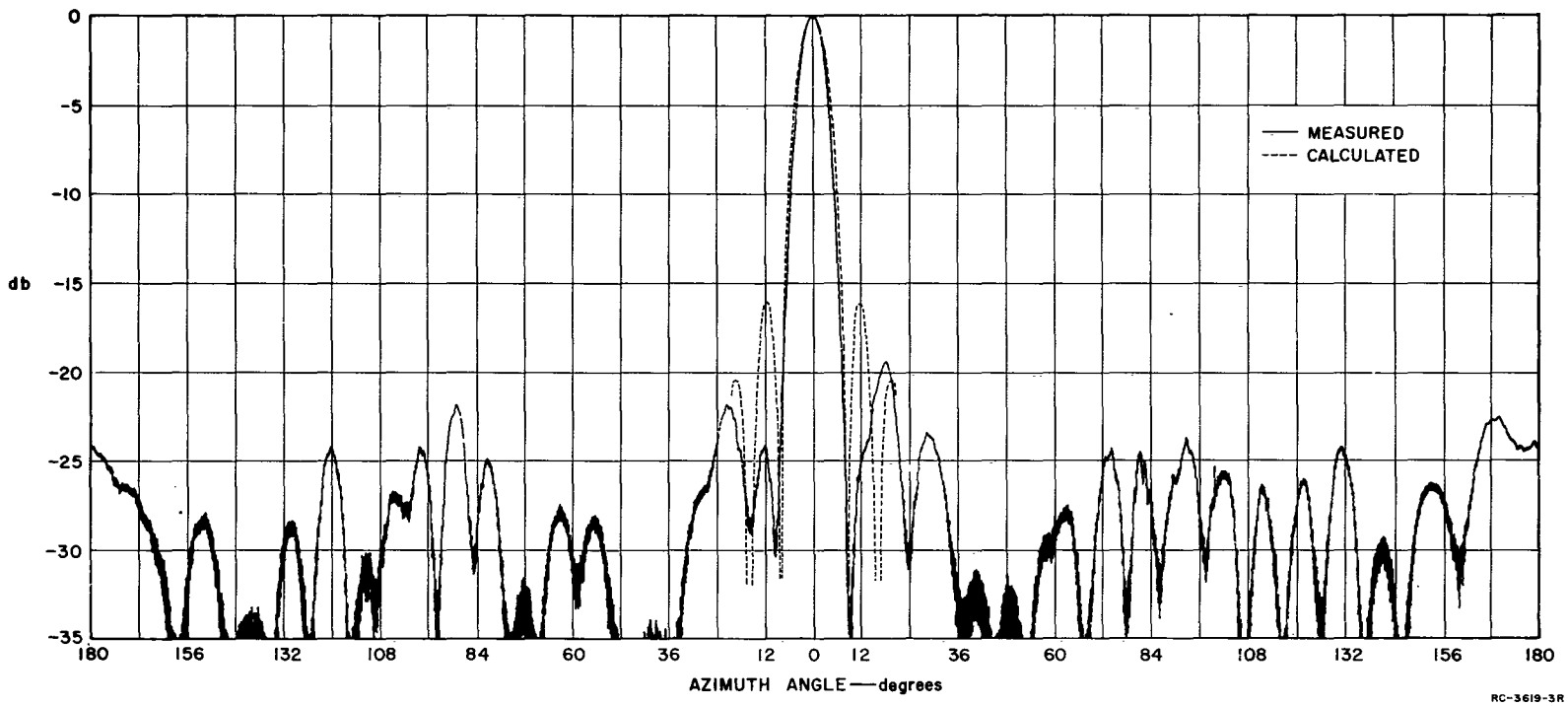

FIG. 23 AZIMUTH RADIATION PATTERN OF EXPERIMENTAL LENS ANTENNA WITH DIRECTIONAL FEED–PRINCIPAL DIRECTION PARALLEL TO GRID WIRES, f = 1.17, ELEVATION ANGLE = 7°, FREQUENCY = 1500 Mc

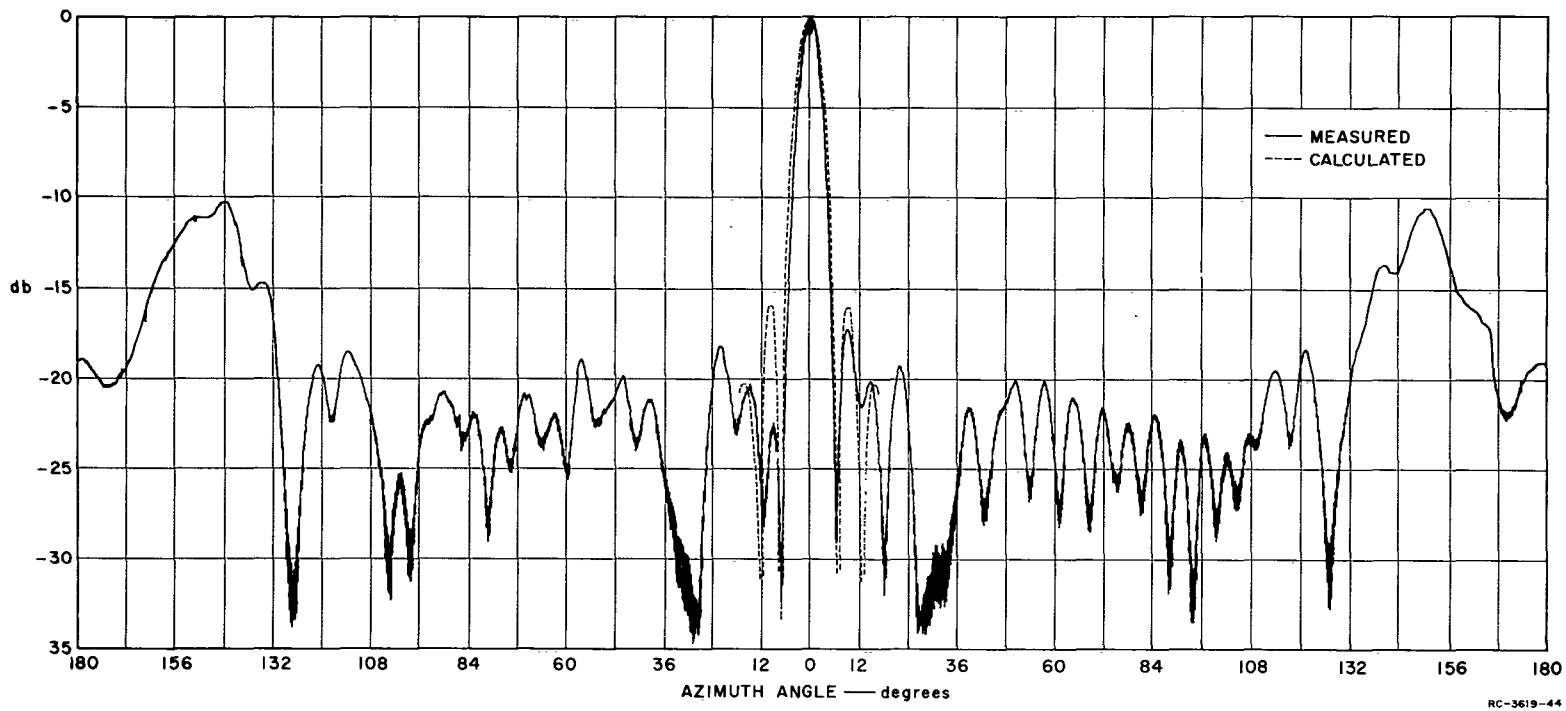

FIG. 24 AZIMUTH RADIATION PATTERN OF EXPERIMENTAL LENS ANTENNA WITH DIRECTIONAL FEED–PRINCIPAL DIRECTION DIAGONAL TO GRID WIRES, f = 1.27, ELEVATION ANGLE = 7°, FREQUENCY = 1750 Mc

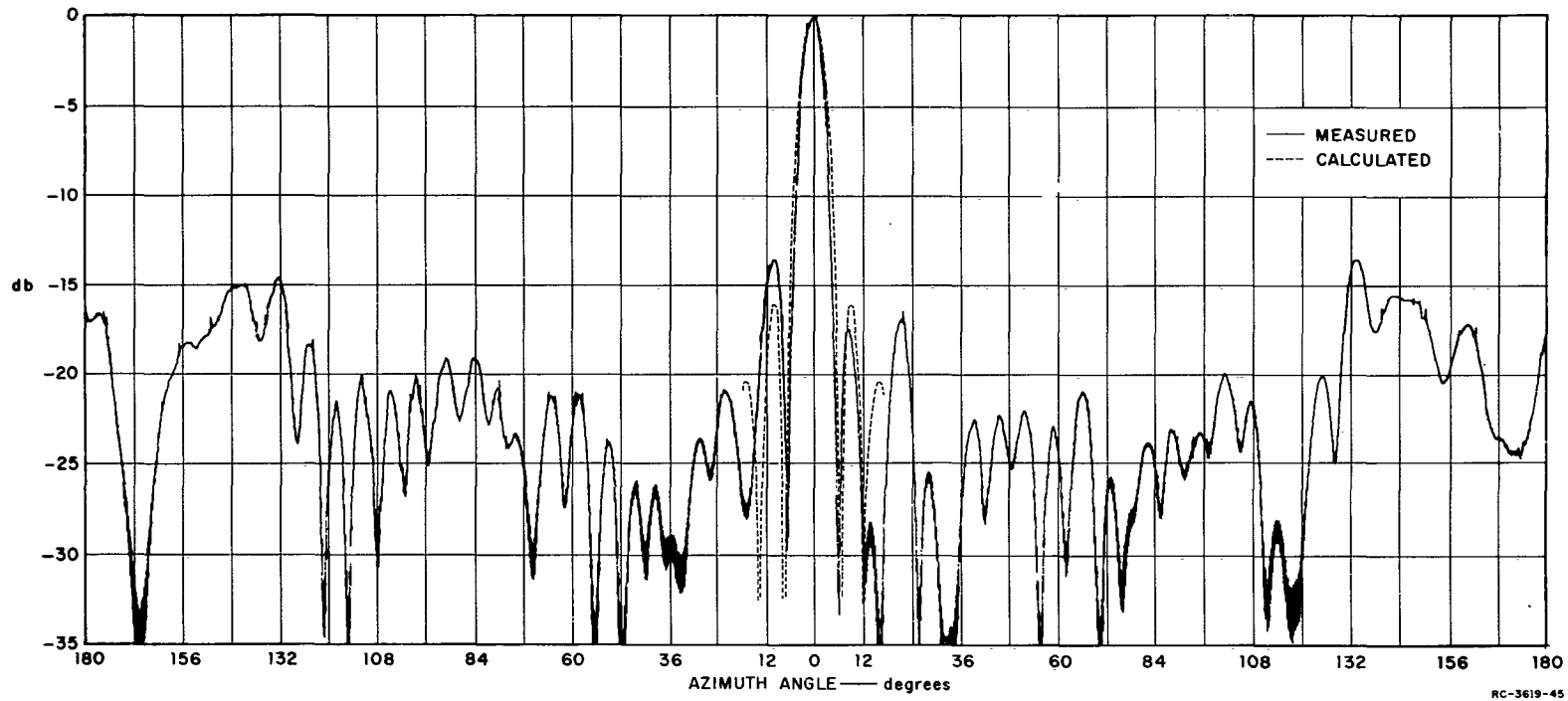

FIG. 25 AZIMUTH RADIATION PATTERN OF EXPERIMENTAL LENS ANTENNA WITH DIRECTIONAL FEED–PRINCIPAL DIRECTION PARALLEL TO GRID WIRES, f = 1.23, ELEVATION ANGLE = 7°, FREQUENCY = 1750 Mc

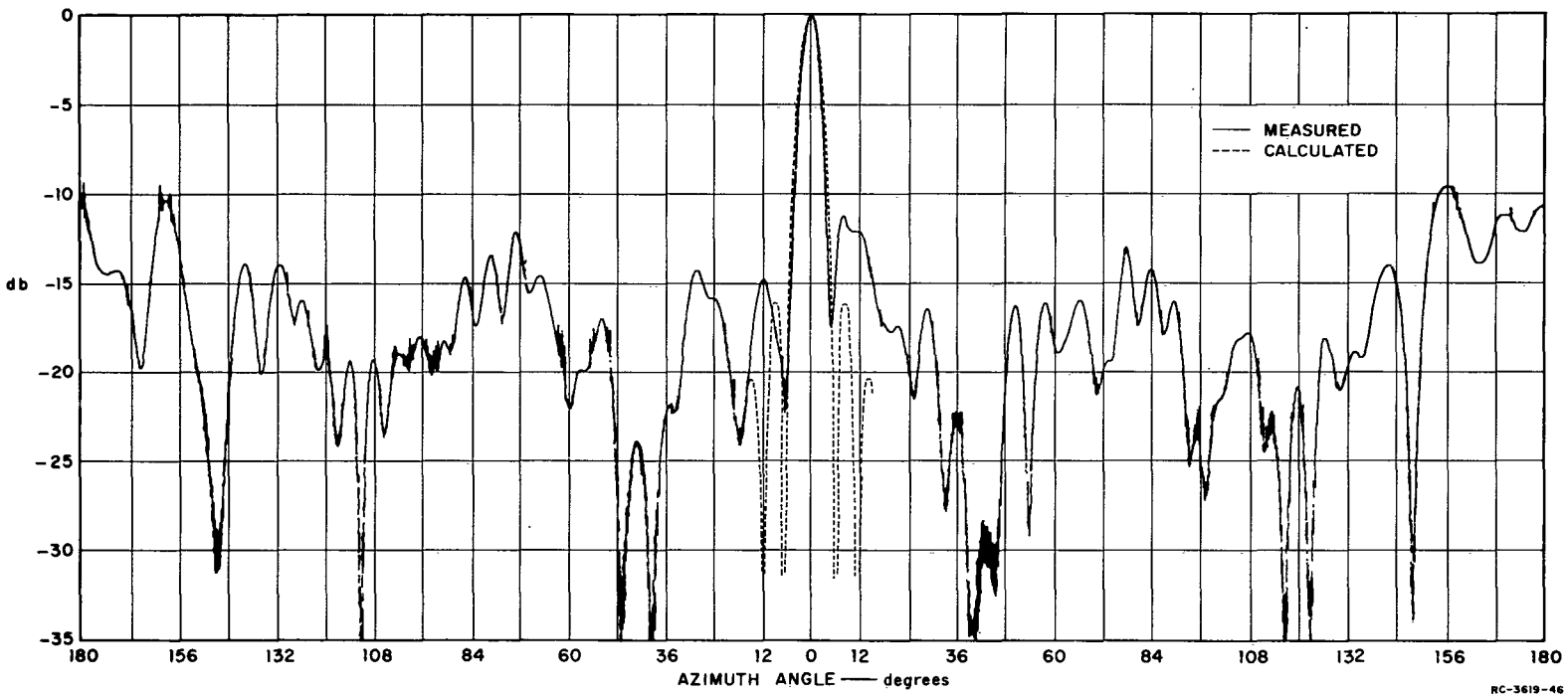

FIG. 26 AZIMUTH RADIATION PATTERN OF EXPERIMENTAL LENS ANTENNA WITH DIRECTIONAL FEED–PRINCIPAL DIRECTION DIAGONAL TO GRID WIRES, f = 1.20, ELEVATION ANGLE = 7°, FREQUENCY = 2000 Mc

frequencies at which the lens was tested. At 1750 Mc, the suppression is not quite effective in directions making an angle of about 35 degrees with the direction opposite to the principal direction of the lens antenna. The poor field suppression in this angular region at 1750 Mc is probably due to the rather strong back lobes of the feed in this region (Fig. 12), and the effect of these back lobes is presumably further enhanced at this frequency by reflection at the conical horn surface. With a more suitable feed than the simple Yagi antenna that was used, this back radiation can probably be suppressed considerably.

To illustrate the effect upon the lens radiation pattern of moving the feed far away from its optimum position, the azimuth radiation pattern of the lens antenna was measured at 1000 Mc with the omnidirectional feed placed in a position corresponding to f = 1.34. This pattern is shown in Fig. 27 and exhibits the expected filling-in of the nulls due to the phase error produced in the plane aperture in front of the lens. The corresponding radiation pattern for the feed placed in the optimum position was shown in Fig. 15.

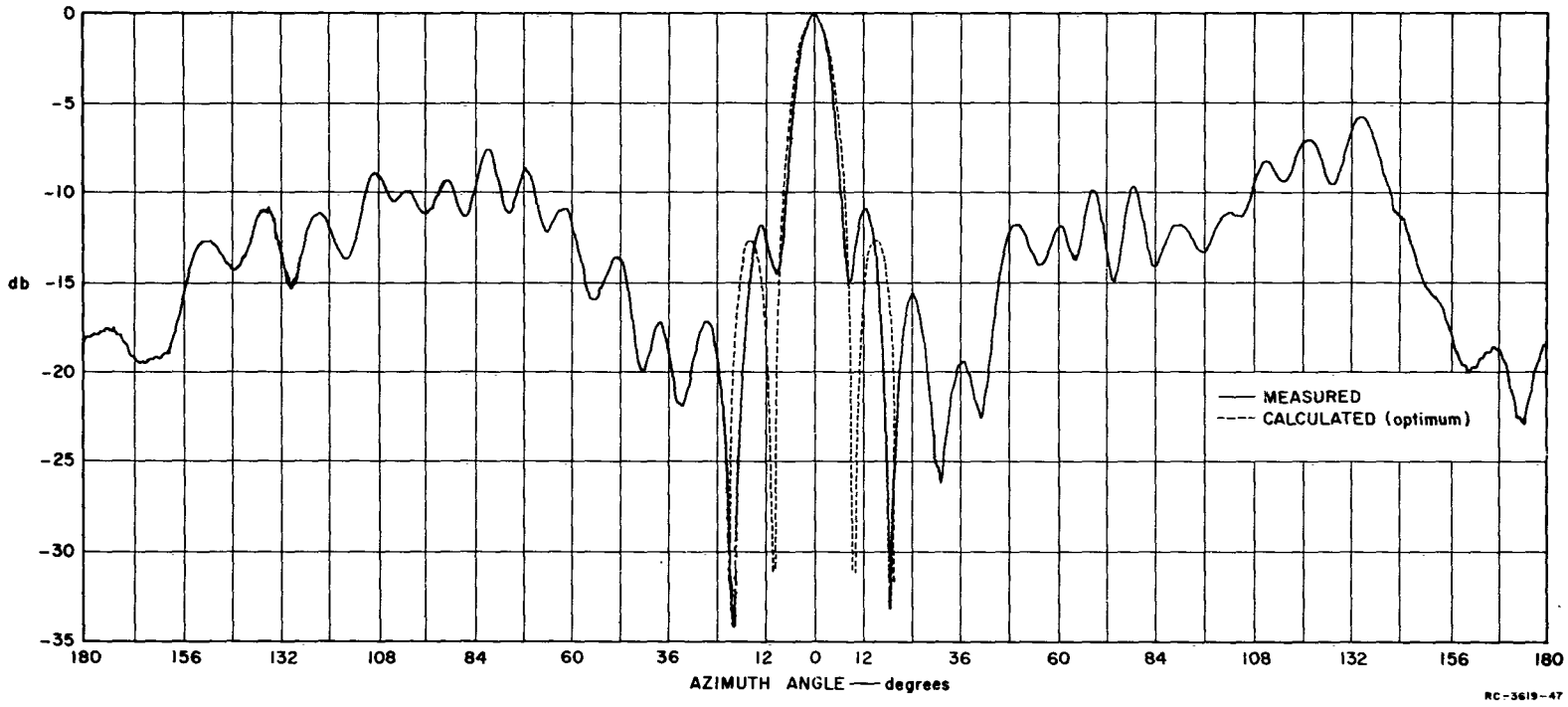

FIG. 27 AZIMUTH RADIATION PATTERN OF EXPERIMENTAL LENS ANTENNA WITH OMNIDIRECTIONAL FEED DISPLACED FROM FOCAL POINT–PRINCIPAL DIRECTION PARALLEL TO GRID WIRES, f = 1.34, ELEVATION ANGLE = 7°, FREQUENCY = 1000 Mc

V CONCLUSION

The measurements on the experimental square-mesh wire-grid modified Luneburg lens antenna have clearly demonstrated the feasibility of using a pair of wire grids (or one wire grid above a ground plane) for Luneburg-type lens antennas. The good agreement between the measured radiation patterns and the theoretical patterns proves the validity of the design formulas that were used for designing the lens antenna and for predicting its radiation pattern.

In conclusion, it should be pointed out that the main purpose of this work has been to demonstrate the feasibility of using a pair of wire grids for a lens antenna. The 2:1 bandwidth and -20 db side-lobe level that were obtained for the experimental square-mesh wire-grid lens antenna do not represent the best results that can be achieved with a wire-grid lens antenna. In principle, the bandwidth of a wire-grid lens antenna can be made as large as desired by using a sufficiently small mesh size of the grid, and the side-lobe level can be reduced below -20 db by using the proper directional feed for the lens. Work that is now under way shows that the square-mesh is really not the best mesh structure to use in a wire-grid lens. A wire-grid lens with hexagonal meshes or triangular meshes will be much less anisotropic and dispersive than a lens with a square-mesh grid and can therefore be used in a larger bandwidth for the same area of the basic mesh.

REFERENCES

1. R. K. Luneburg, "Mathematical Theory of Optics," Lecture notes from Brown University Graduate School, Providence, Rhode Island, 1944.

2. S. P. Morgan, "General Solution of the Luneburg Lens Problem," J. Appl. Physics, 29, pp. 1358-1368 (September 1958).

3. H. Jasik, "The Electromagnetic Theory of the Luneburg Lens," Antenna Laboratory, Electronics Research Directorate, Air Force Cambridge Research Center, Cambridge, Massachusetts. (November 1954) AFCRD-TR-54-121.

4. C. T. Tai, "Theory of the Cylindrical Luneburg Lens Excited by a Line Magnetic Current," Contract AF 19(604) 1725, Report No. 678-3, Antenna Lab., Ohio State University (September 15, 1956).

5. G. D. M. Peeler and D. H. Archer, "A Two-Dimensional Microwave Luneburg Lens," NRC Report 4115, Naval Research Laboratory, Washington, D.C. (March 1953).

6. S. Adachi and C. H. Walter, "A Spherical Cap Lens," Report 903-3, Contract AF 33(616)-6211, Ohio State University, Columbus, Ohio (April 1959).

7. S. Adachi, R. C. Rudduck and C. H. Walter, "A General Analysis of Non-Planar Two-Dimensional Luneburg Lenses," Report 903-10, Contract AF 33(616)-6211, Ohio State University, Columbus, Ohio (June 1960).

8. C. H. Walter, "Surface-Wave Luneburg Lens Antennas," IRE Trans. PGAP-8, pp. 508-515 (September 1960).

9. R. L. Tanner, "New Ideas in HF Antennas," paper presented orally at a PGAP Meeting at Stanford University in January 1960.

10. M. G. Andreasen, P. S. Carter, and W. F. Gabriel, "Investigation of Methods of Scanning the Beam of Large Antennas," SRI Project 2184, Final Report, Part I, Contract AF 19(604)-2240, Stanford Research Institute, Menlo Park, California (March 1961).

11. M. G. Andreasen and R. L. Tanner "Properties of a Pair of Wire Grids for Use in Lens-Type HF Antennas," Paper presented at WESCON, August 1961.

12. D. K. Cheng, "Modified Luneburg Lens for Defocused Source," IRE Trans. PGAP-8, pp. 110-111 (January 1960).

13. E. T. Copson, Theory of Functions of a Complex Variable (Oxford University Press, London, 1935).

STANFORD RESEARCH INSTITUTE | MENLO PARK, CALIFORNIA

Regional Offices and Laboratories

SOUTHERN CALIFORNIA LABORATORIES
820 Mission Street
South Pasadena, California

WASHINGTON OFFICE
808 17th Street, N.W.
Washington 5, D.C.

NEW YORK OFFICE
270 Park Avenue, Room 1770
New York 17, New York

DETROIT OFFICE
The Stevens Building
1025 East Maple Road
Birmingham, Michigan

EUROPEAN OFFICE
Pelikanstrasse 37
Zurich 1, Switzerland

Representatives

HONOLULU, HAWAII
Finance Factors Building
195 South King Street
Honolulu, Hawaii

LONDON, ONTARIO, CANADA
85 Wychwood Park
London, Ontario, Canada

LONDON, ENGLAND
15 Abbotsbury Close
London W. 14, England

MILAN, ITALY
Via Macedonio Melloni 40
Milano, Italy